Geological Society of America Bulletin

# Eocene–Oligocene global climate and sea-level changes: St. Stephens Quarry, Alabama

Kenneth G. Miller, James V. Browning, Marie-Pierre Aubry, Bridget S. Wade, Miriam E. Katz, Andrew A. Kulpecz and James D. Wright

*Geological Society of America Bulletin* 2008;120, no. 1-2;34-53
doi: 10.1130/B26105.1

# Eocene–Oligocene global climate and sea-level changes: St. Stephens Quarry, Alabama

**Kenneth G. Miller***
**James V. Browning**
**Marie-Pierre Aubry**
**Bridget S. Wade**[§]
**Miriam E. Katz**[†]
**Andrew A. Kulpecz**
**James D. Wright**
*Department of Geological Sciences, Rutgers University, Piscataway, New Jersey 08854, USA*

## ABSTRACT

**We integrate upper Eocene–lower Oligocene lithostratigraphic, magnetostratigraphic, biostratigraphic, stable isotopic, benthic foraminiferal faunal, downhole log, and sequence stratigraphic studies from the Alabama St. Stephens Quarry (SSQ) core hole, linking global ice volume, sea level, and temperature changes through the greenhouse to icehouse transition of the Cenozoic. We show that the SSQ succession is dissected by hiatuses associated with sequence boundaries. Three previously reported sequence boundaries are well dated here: North Twistwood Creek–Cocoa (35.4–35.9 Ma), Mint Spring–Red Bluff (33.0 Ma), and Bucatunna-Chickasawhay (the mid-Oligocene fall, ca. 30.2 Ma). In addition, we document three previously undetected or controversial sequences: mid-Pachuta (33.9–35.0 Ma), Shubuta-Bumpnose (lowermost Oligocene, ca. 33.6 Ma), and Byram-Glendon (30.5–31.7 Ma). An ~0.9‰ $\delta^{18}O$ increase in the SSQ core hole is correlated to the global earliest Oligocene (Oi1) event using magnetobiostratigraphy; this increase is associated with the Shubuta-Bumpnose contact, an erosional surface, and a biofacies shift in the core hole, providing a first-order correlation between ice growth and a sequence boundary that indicates a sea-level fall. The $\delta^{18}O$ increase is associated with a eustatic fall of ~55 m, indicating that ~0.4‰ of the increase at Oi1 time was due to temperature. Maximum $\delta^{18}O$ values of Oi1 occur above the sequence boundary, requiring that deposition resumed during the lowest eustatic lowstand. A precursor $\delta^{18}O$ increase of 0.5‰ (33.8 Ma, mid-chron C13r) at SSQ correlates with a 0.5‰ increase in the deep Pacific Ocean; the lack of evidence for a sea-level change with the precursor suggests that this was primarily a cooling event, not an ice-volume event. Eocene–Oligocene shelf water temperatures of ~17–19 °C at SSQ are similar to modern values for 100 m water depth in this region. Our study establishes the relationships among ice volume, $\delta^{18}O$, and sequences: a latest Eocene cooling event was followed by an earliest Oligocene ice volume and cooling event that lowered sea level and formed a sequence boundary during the early stages of eustatic fall.**

**Keywords:** Eocene-Oligocene, sea level, climate, ice volume, Alabama, sequence stratigraphy, icehouse, greenhouse.

## INTRODUCTION

The Eocene–Oligocene transition (ca. 35–33 Ma) was the most profound oceanographic and climatic change of the past 50 m.y. (e.g., Miller, 1992; Zachos et al., 2001). A global earliest Oligocene (33.55 Ma) $\delta^{18}O$ increase of 1.0‰–1.5‰ (Oi1 of Miller et al., 1991) occurred throughout the Atlantic, Pacific, Indian, and Southern Oceans (Shackleton and Kennett, 1975; Savin et al., 1975; Kennett and Shackleton, 1976; Keigwin, 1980; Corliss et al., 1984; Miller et al., 1987; Zachos et al., 2001; Coxall et al., 2005). Most studies agree that the earliest Oligocene marked the beginning of the icehouse Earth, with large (i.e., near modern sized) ice sheets in Antarctica (e.g., Miller et al., 1991; Zachos et al., 1992). However, considerable controversy has surrounded the cause of the $\delta^{18}O$ increase that culminated in Oi1, ranging from early studies that attribute it entirely to a cooling of deep-water (and hence, high-latitude surface water) temperatures (Shackleton and Kennett, 1975; Savin et al., 1975; Kennett and Shackleton, 1976), to a recent study that attributes the entire 1.5‰ $\delta^{18}O$ increase observed in the deep Pacific to growth of ice sheets (Tripati et al., 2005). This latter interpretation requires: (1) ice storage that is ~1.5 times that of modern ice sheets; (2) the presence of large ice sheets in Antarctica and in the Northern Hemisphere; and (3) a global sea-level (eustatic) fall of ~150 m. It is based on the lack of a deep-sea Mg/Ca change associated with the Oi1 $\delta^{18}O$ increase (Lear et al., 2000), implying little or no cooling. However, a dramatic drop in the calcite compensation depth occurred at this transition (Van Andel et al., 1975; Coxall et al., 2005), and may have caused changes in carbonate ion activity that masked cooling in Mg/Ca records (Lear et al., 2004).

There is ample evidence for a major global cooling during the Eocene–Oligocene transition. Paleontological evidence for cooling includes the development of psychrospheric (cold-loving) ostracods (Benson, 1975), a deep-sea benthic foraminiferal turnover (e.g., Miller et al., 1992; Thomas, 1992), the loss of calcareous nannoplankton that thrived in early Paleogene warm, oligotrophic waters (Aubry, 1992), regional evidence for cooling from pollen (e.g., New Jersey; Owens et al., 1988), mammalian turnover (e.g., England; Hooker et al., 2004), and microfossil assemblages (e.g.,

*kgm@rci.rutgers.edu
[§]Present address: Department of Geology and Geophysics, Texas A&M University, College Station, Texas 77843, USA
[†]Also at: Earth and Environmental Sciences, Rensselaer Polytechnic Institute, Troy, New York 12180, USA

*GSA Bulletin*; January/February 2008; v. 120; no. 1/2; p. 34–53; doi: 10.1130/B26105.1; 9 figures; Data Repository Item 2007208.

New Zealand; Nelson and Cook, 2001). Isotopic evidence also indicates global cooling. The $\delta^{18}O$ increase in the deep Atlantic is typically 1.0‰ (e.g., Miller and Curry, 1982); the 1.5‰ $\delta^{18}O$ increase at Ocean Drilling Program (ODP) Site 1218 (deep Pacific; Coxall et al., 2005) implies that there was at least a 2 °C cooling in the deep Pacific. Comparisons of benthic foraminiferal $\delta^{18}O$ records and a latitudinal profile of planktonic foraminiferal $\delta^{18}O$ values show a shift in mean values of ~0.6‰ from the late Eocene to the early Oligocene (Keigwin and Corliss, 1986). This global change in $\delta^{18}O_{seawater}$ is best explained by ice growth with a consequent sea-level lowering of ~50–60 m (using the $\delta^{18}O$/sea level calibrations of Fairbanks and Matthews [1978] and Pekar et al. [2002] of 0.11‰/10 m and 0.1‰/10 m, respectively). Nevertheless, the precise amount of the $\delta^{18}O$ increase that is attributable to ice versus temperature remains debatable.

Sea-level studies have established that a major eustatic drop occurred in the earliest Oligocene. Although the Exxon Production Research Company (Exxon) sea-level curve shows no earliest Oligocene change and a dramatic (160+ m) mid-Oligocene fall (Vail et al., 1977; Haq et al., 1987), studies in New Jersey have documented a major earliest Oligocene eustatic fall of ~55 m (Pekar et al., 2001; Miller et al., 2005a). Using the sea level/$\delta^{18}O_{seawater}$ calibrations cited above, this implies that ~0.5‰–0.6‰ of the deep-sea $\delta^{18}O$ increase was due to an increase in ice volume and ~0.5‰–1.0‰ was due to a 2–4 °C deep-water cooling. Sequence stratigraphic and backstripping studies in New Jersey have documented that the mid-Oligocene eustatic lowering was ~50–60 m (Pekar et al., 2001; Miller et al., 2005a), far less than the 160 m fall shown by the Exxon curves. The absence of an earliest Oligocene event on the Exxon curve has been a source of discussion and debate for more than 25 yr (Olsson et al., 1980).

Until now, the data sets used to decipher ice-volume changes across the Eocene–Oligocene transition were derived from deep-sea locations largely drilled by the Deep Sea Drilling Project and the ODP. In contrast, sea-level studies of this interval have mostly examined seismic profiles on continental margins (e.g., Vail et al., 1977) or marine sections on land (e.g., Vail et al., 1987; Haq et al., 1987; Loutit et al., 1988; Baum and Vail, 1988; Miller et al., 2005a). It has proven difficult to obtain expanded and reliable $\delta^{18}O$ records for onshore marine sections because of hiatuses, diagenesis, poorly fossiliferous sections, and other complications due to nearshore influences. Linking deep-sea isotopes and sea-level records requires using magnetobiostratigraphic correlations that have errors of 0.5–1.0 m.y. (e.g., Miller et al., 1990). Miller et al. (1998) provided first-order correlations between Miocene sequences and $\delta^{18}O$ records at New Jersey continental slope Site 904, directly linking $\delta^{18}O$ increases and sequence boundaries. Such comparisons provide a prima facie link between ice volume and sequences, but such first-order correlations for the Eocene and Oligocene have been lacking until this study.

St. Stephens Quarry (SSQ) in Alabama has provided one of the global reference sections for the Eocene–Oligocene transition, yet the basic relationships among sequences, sea level, temperature, and biotic events in this section have been controversial. Pioneering sequence stratigraphic studies of the SSQ outcrop were published as part of the Exxon sea-level curve (Baum and Vail, 1988; Loutit et al., 1988; Fig. 1). SSQ outcrop studies have integrated sequence stratigraphy with planktonic foraminiferal biostratigraphy (Mancini and Tew, 1991; Tew, 1992). Keigwin and Corliss (1986) identified a major (~1‰) $\delta^{18}O$ increase in the lowermost Oligocene in the SSQ outcrop. ARCO Oil and Gas Company drilled a core hole at SSQ in 1987 that spanned the Eocene–Oligocene section and yielded an unambiguous magnetostratigraphy for the core hole reported by Miller et al. (1993). There is general agreement among studies of SSQ, both outcrop and core hole (Fig. 1), except for one critical interpretation: is there an earliest Oligocene sequence boundary and an attendant sea-level fall? One school maintains that the lowermost Oligocene Shubuta-Bumpnose formational contact at SSQ and elsewhere in Alabama and Mississippi is associated with a maximum flooding surface (MFS) of a sequence (Baum and Vail, 1988; Loutit et al., 1988; Mancini and Tew, 1991; Tew, 1992; Jaramillo and Oboh-Ikuenobe, 1999; Echols et al., 2003). A second school maintains that there is a sequence boundary at this level (Dockery, 1982) and associates the contact with a $\delta^{18}O$ increase (Keigwin and Corliss, 1986) and attendant sea-level fall (Miller et al., 1993). It has been difficult to choose between these hypotheses because of the lack of critical data sets (e.g., log data, benthic foraminiferal biofacies, and $\delta^{18}O$). The presence or absence of a sequence boundary at the time of the global earliest Oligocene $\delta^{18}O$ increase has profound implications for the role of temperature versus ice volume at this time.

In this paper we revisit the upper Eocene–middle Oligocene portion of the SSQ core hole. We describe the lithologic units in the

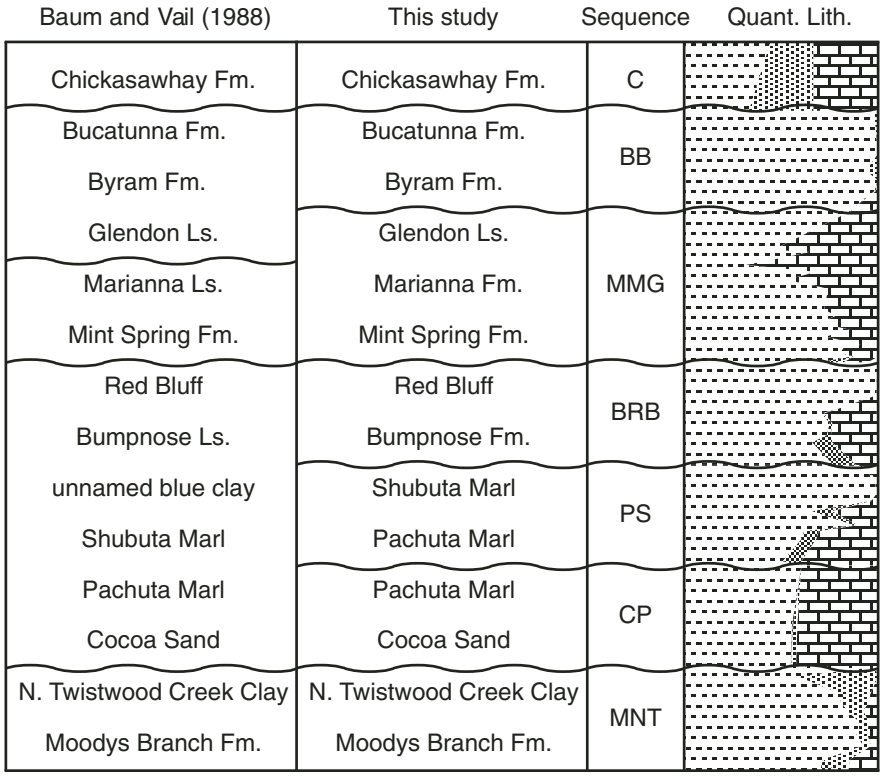


**Figure 1. Comparison of the sequence stratigraphic interpretation of Baum and Vail (1988) and this study. Quantitative lithology (total = 100%) is derived from the data from the core hole presented here. See Figure 2 for lithology key.**

core hole, conduct a detailed sequence stratigraphic description of the upper Eocene to mid-Oligocene section, and generate the following new data sets on the SSQ core hole: quantitative lithology, benthic foraminiferal biofacies, planktonic microfossil biostratigraphy, gamma log, and benthic foraminiferal stable isotopes. We integrate these results with published magnetostratigraphic and biostratigraphic data summarized by Miller et al. (1993), thus providing first-order correlations between stable isotopic and sequence stratigraphic data spanning the Eocene–Oligocene transition. We then compare these integrated sequence and isotopic records at SSQ with the well-dated (age control better than 0.5 m.y.) upper Eocene–Oligocene sequence stratigraphic records from New Jersey and with the most detailed deep-sea stable isotopic records available from Pacific Site 1218 (Coxall et al., 2005). These well-dated records show remarkably similar patterns that allow comparison of strata in different tectonic and sedimentological settings and with the $\delta^{18}O$ proxy for glacioeustasy.

## METHODS

### Core Holes and Correlations

SSQ (Fig. 2) was continuously cored by ARCO Oil and Gas Company in 1987. Magnetostratigraphic and Sr isotopic studies were reported along with biostratigraphic results by Miller et al. (1993). The SSQ core hole was recently archived in the Rutgers Core Repository (http://geology.rutgers.edu/corerepository/index.html) by G. Baum and G. Keller. An analog gamma log (G. Baum, 2004, personal commun.) was digitized (Fig. 2). We examined calcareous nannofossil and planktonic foraminiferal biostratigraphy and benthic foraminiferal biofacies successions from splits of the original magnetostratigraphic (Figs. 2–4) samples from the SSQ core hole (Fig. 2), and obtained additional samples for planktonic microfossil stratigraphy and stable isotopic studies. The core hole was logged in feet (ft) and we retain these units to maintain consistency among closely spaced samples (but supply metric conversions to all samples). Samples for lithofacies and benthic foraminiferal biofacies analysis were taken at a sampling interval of ~1–5 ft (0.3–1.5 m), and the core was redescribed for lithology and sequence stratigraphy. Detailed procedures for each type of analysis are provided in the following.

We compare the SSQ core hole results to results from the New Jersey coastal plain (Fig. 5). The ACGS#4 core hole was drilled by the U.S. Geological Survey and the New Jersey Geological Survey near Mays Landing, New Jersey, in 1984 (Fig. 5; Owens et al., 1988) and analyzed for magnetostratigraphy and Sr isotope stratigraphy by Miller et al. (1990). The Island Beach core hole was drilled as a part of ODP Leg 150X (Miller et al., 1994, 1996; Fig. 5). Oligocene and upper Eocene sequence stratigraphy for the Island Beach core hole were summarized by Pekar et al. (1997) and Browning et al. (1997), respectively.

Sequences in both Alabama and New Jersey were dated using integrated stratigraphy, including foraminiferal and calcareous nannoplankton stratigraphy, magnetostratigraphy, and Sr isotopic stratigraphy (Poore and Bybell, 1988; Miller et al., 1993, 1994, 1996; Pekar et al., 1997; Browning et al., 1997). Correlation to the Berggren et al. (1995) time scale relies primarily on the excellent magnetostratigraphic records available (Figs. 3–5; van Fossen [1997] for New Jersey; Miller et al. [1993] for Alabama).

### Lithofacies

Upper Eocene–Oligocene outcrop and subsurface strata in Alabama consist of the following well-known Gulf Coast lithostratigraphic units (Toulmin, 1977; Baum and Vail, 1988; Tew, 1992; Tew and Mancini, 1995).

1. The Jackson Stage (approximately upper Eocene) comprises the Moodys Branch Formation, North Twistwood Creek Clay, and Yazoo Formation and its members, the Cocoa Sand, Pachuta Marl, and Shubuta Clay.

2. The Vicksburg Stage (approximately lower Oligocene) comprises the laterally equivalent Forest Hill Sand–Red Bluff–Bumpnose Formations, informal Mint Spring formation, Marianna Limestone, and the Byram Formation, including the Bucatunna Clay Member.

3. The Chickasawhay Stage (approximately mid-Oligocene) comprises the Chickasawhay Formation.

D.T. Dockery (1989, personal commun.) identified the depths of lithologic units in the SSQ core hole as reported in Miller et al. (1993). However, examination of the core hole shows that there are some minor discrepancies in the depths of the core as reported by Dockery. We reinterpreted the depths in the core to standardize measurement; this results in minor shifts (to 0.5 ft [15 cm]) in the depths of the lithologic contacts.

We used lithofacies (% sand fraction, % glauconite, relative abundance of carbonates versus siliciclastics), percent planktonic foraminifera, and benthic foraminiferal faunal data to infer paleoenvironmental changes between and within sequences (Figs. 2 and 3). Samples of ~20 $cm^3$ were soaked in a sodium metaphosphate solution to disaggregate the sediment. A few samples required heating in a sodium carbonate solution. Samples were washed through a 63 µm mesh to remove the clay and silt, and the percent sand was computed. The percent glauconite and relative abundances of carbonates versus quartz sand were visually estimated. Glauconite is associated with intervals of low sedimentation rates, usually associated with transgressive systems tracts (TST). Quartz sand increases in highstand systems tracts (HST) in many sequences globally, but here we observe this pattern only in the shallowest sequence (Moodys–North Twistwood Creek). Carbonate in the sand fraction (Fig. 2) is composed of foraminifer and mollusk fragments and shows a less predictable relationship to sequences; it is inversely proportional to the mud fraction (Fig. 2) that tends to increase in the upper HST of two sequences (i.e., HST quartz sands are absent).

### Biostratigraphy

#### *Calcareous Nannofossils*

Smear slides were prepared from sediment in the interval between 271 ft (82.6 m; in the Moodys Branch Formation) and 73 ft (22.5 m; in the Marianna Formation). An additional sample was taken at 14 ft (4.27 m) from the Chickasawhay Formation. Sample density is high (1–3 ft; 0.31–0.81 m) in the Pachuta Marl to the base of the Marianna Formation interval (178–129 ft; 54.25–39.32 m) and much lower (~8 ft; 2.44 m) below the Pachuta and in the bulk of the Marianna Formation. Slides were studied with a Zeiss microscope at 500–1200× magnification. Special attention was given to determine the stratigraphic distribution of the (often scarce) primary and secondary biozonal markers (Martini, 1971; Berggren et al., 1995), while the species inventory helped to determine levels where markers are reworked.

#### *Planktonic Foraminifera*

Samples for foraminiferal biostratigraphy were taken from the paleomagnetic samples (Miller et al., 1993) supplemented by additional 20 $cm^3$ samples for a total of 83 samples from 75 to 230 ft (22.86–70.10 m). The >63 µm fraction was dry sieved into three different size fractions, which were studied for their foraminiferal assemblages: 63–125 µm, 125–250 µm, and >250 µm.

### Benthic Foraminiferal Biofacies

After washing, the dried samples from SSQ were sieved to obtain the >105 µm fraction and random samples of ~300 specimens were picked for quantitative benthic foraminiferal

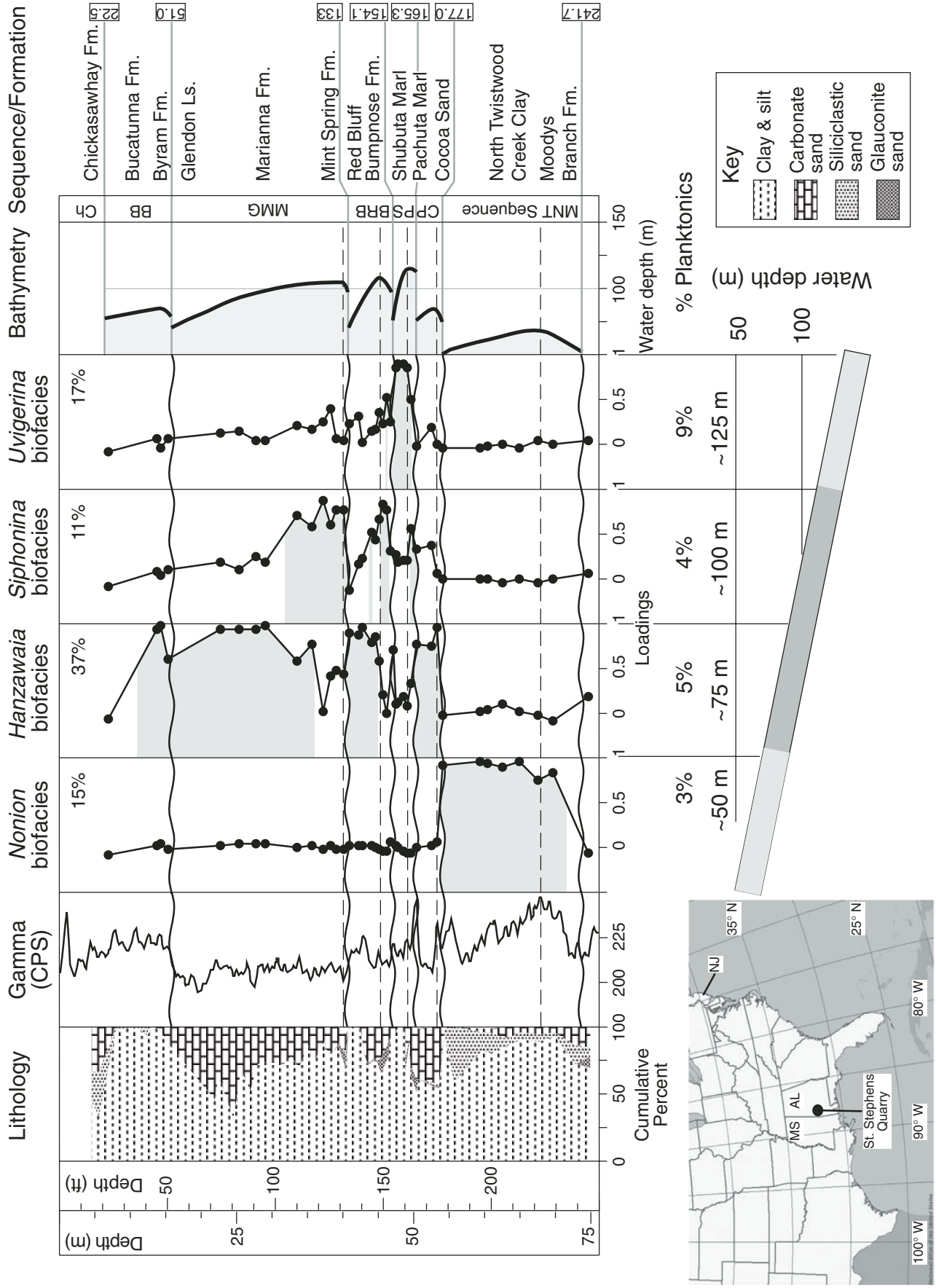


**Figure 2. Distribution of benthic foraminiferal factor loadings calculated for the SSQ core hole. Shaded areas represent sediments where a particular factor is significant. Below is the depth model developed for the benthic foraminiferal biofacies. Inset is a map showing the location of the St. Stephens Quarry, Alabama (AL), core hole. Gamma log and lithology are shown on left. CPS—counts per second; Fm—formation; Ls—limestone; MS—Mississippi; NJ—New Jersey.**

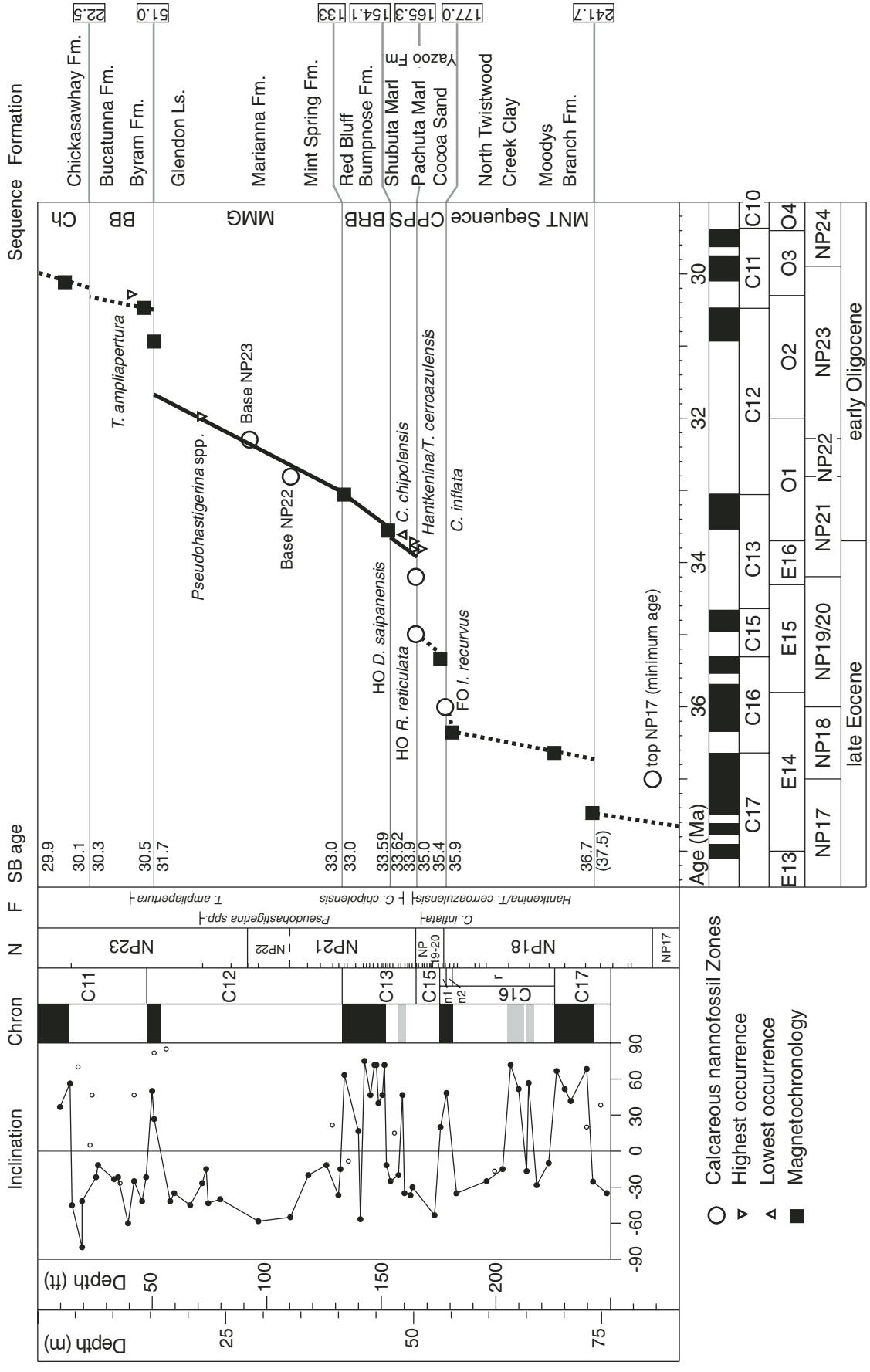


**Figure 3. Age-depth diagram for the St. Stephens Quarry, Alabama, core hole. Inclination data are from Miller et al. (1993); chron, foraminiferal (F), and nannofossil (N) interpretations are from this study. Solids symbols are magnetochrons. Chronozones—C16, C15r. Open symbols are foraminiferal (triangle indicates lowest occurrence [LO]; inverted triangle indicates highest occurrence [HO]) and nannofossil (circles) datum levels. SB—sequence boundary with ages derived from the plot. Time scale of Berggren et al. (1995; BKSA95). Solid horizontal lines are sequence boundaries. Fm—formation; Ls—limestone. *I.—Isthmolithus*; *T.—Turborotalia*; *R.—Reticulofenestra*; *D.—Discoaster*; *C.—Chiasmolithus*.**

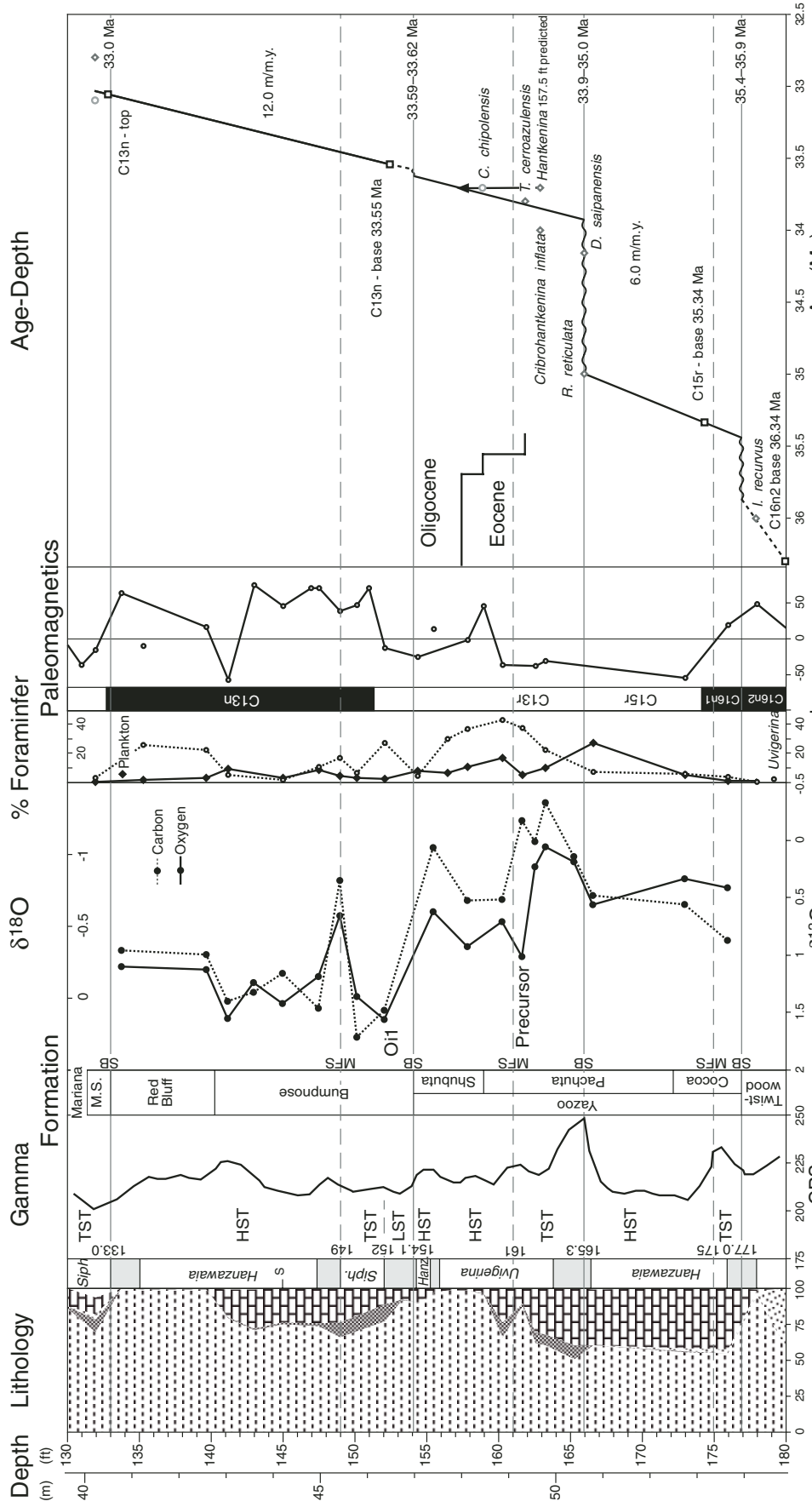


**Figure 4. Enlargement of integrated lithology, biofacies, gamma log, stable isotopes, magnetostratigraphy, and age-depth plot for the uppermost Eocene–lowermost Oligocene. Oi1—Oligocene isotope maximum 1; TST—transgressive systems tract; HST—highstand systems tract. Chronozones—C16, C15r. Isotope values are relative to Vienna Peedee belemnite (VPDB, ‰). Lithology key is in Figure 2. CPS—counts per second. Stairstep line indicates uncertainties in placement of the Eocene-Oligocene boundary with preferred placement at longest line. Shaded intervals between biofacies are sampling gaps. Time scale of Berggren et al. (1995; BKSA95). Solid horizontal lines are sequence boundaries (SB), dashed lines are maximum flooding surfaces (MFS), wavy lines are hiatuses.**

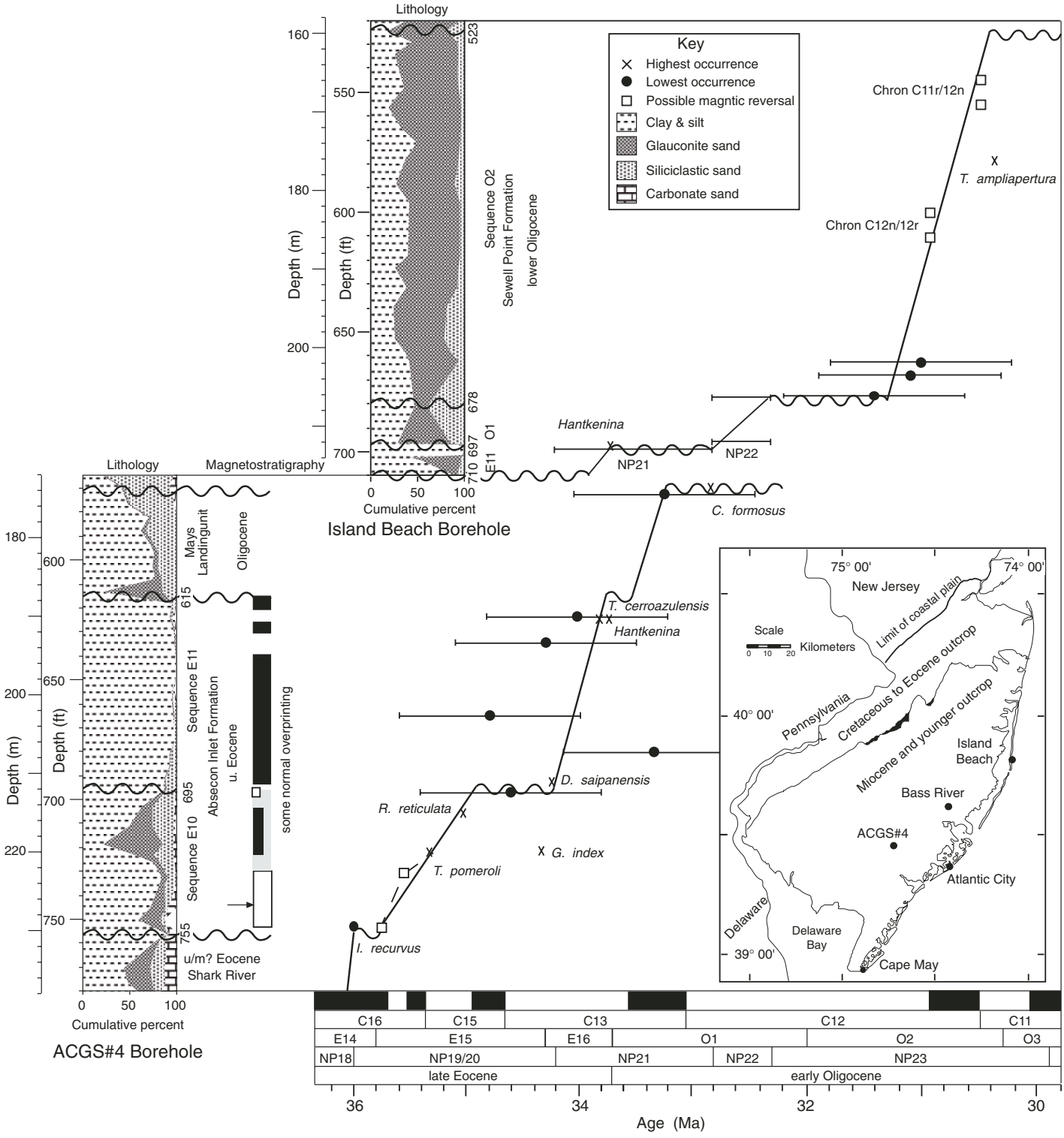


**Figure 5. Age-depth diagram for the ACGS#4 and Island Beach, New Jersey, core holes. Black dots with error bars indicate strontium isotopic age estimates. Inset map shows the locations of New Jersey core holes discussed in the text. Polarity interpretation is that of van Fossen (1987). Data are derived from Pekar et al. (1997) and Browning et al. (1997). Time scale of Berggren et al. (1995; BKSA95). *I.—Isthmolithus*; *T.—Turborotalia*; *R.—Reticulofenestra*; *D.—Discoaster*; *C.—Chiasmolithus*; *G.—Globigerinatheka*.**

analysis. Benthic foraminifers were identified to species level using the taxonomy of Tjalsma and Lohmann (1983), Jones (1983), Bandy (1949), Enright (1969), Boersma (1984), and Charletta (1980). The data set was normalized to percentages and Q-mode factor analysis was used to document faunal variations among the samples. The factors obtained were rotated using a Varimax Factor rotation using Systat 5.2.1.

Benthic foraminiferal assemblages were quantitatively characterized and used to interpret depositional environments and to establish water-depth fluctuations (Fig. 2). We examined 39 samples and a total of 70 species were identified from ~9235 specimens (see GSA Data Repository Table DR1[1]). Four Q-mode Varimax factors were extracted from the percentage data, explaining ~80% of the faunal variation (Fig. 2).

### Oxygen Isotopic Records

Benthic foraminiferal stable isotope analyses from the SSQ core hole were generated in the Stable Isotope Laboratory in the Department of Geological Sciences at Rutgers University. We selected ~1–5 specimens of monogeneric benthic foraminifera (*Cibicidoides* spp.) from each sample for analysis (Fig. 4; Table DR2 [see footnote 1]); this genus typically comprises <10% of the ~300 specimens picked for census studies. Although less common than other taxa, we chose this genus because of its consistent occurrence and the fact that its isotopic calibration is well known (e.g., Katz et al., 2003). Foraminifera were reacted in phosphoric acid at 90 °C for 15 min in an automated peripheral attached to a Micromass Optima mass spectrometer. The $\delta^{18}O$ and $\delta^{13}C$ values are reported versus Vienna Peedee belemnite by analyzing NBS-19 or an internal lab standard during each automated run. Typically 8 standards are analyzed along with 32 samples; 1σ precision for standards is 0.08 and 0.05 for $\delta^{18}O$ and $\delta^{13}C$, respectively. Sample resolution in the upper part of chronozone (chron) C13r to C13n is 50 cm (~40 k.y. or better using average sedimentation rates of 1.2 cm/k.y for this section).

Preservation of microfossils varies through the section, from pristine in more clay-rich intervals (e.g., Fig. 6) to moderate in more carbonate-rich intervals. Planktonic stable isotopic and benthic Mg/Ca studies of the SSQ core hole are ongoing, and we discuss only the benthic foraminiferal $\delta^{18}O$ and $\delta^{13}C$ records.

[1]GSA Data Repository Item 2007208, Tables DR1 and DR2, is available at www.geosociety.org/pubs/ft2007.htm. Requests may also be sent to editing@geosociety.org.

## RESULTS

### Benthic Foraminiferal Biofacies and Paleobathymetry

We constructed a paleodepth curve for SSQ biofacies by placing them into a relative depth rank using lithologic (% sand fraction, % glauconite, relative abundance of carbonates versus siliciclastics, nature of bioturbation) and faunal (% planktonic foraminifers, benthic foraminiferal biofacies) criteria (Fig. 2, bottom panel) and by using modern depth distributions to assign water depths (see summary in Douglas, 1979). From shallowest to deepest, these biofacies are as follows.

#### *Nonion Biofacies*

Factor 2 (15% of the variance explained; Fig. 2) is characterized by the common occurrences of *Nonion stavensis*, *Nonionella spiralis*, and *Nonionella spissa*. It is confined to the North Twistwood Creek Clay and associated with sediments containing the highest percentage of siliciclastic sand. The *Nonion* biofacies is the shallowest biofacies (~50 m water depth), based on the lowest percent planktonic foraminifers (3%) and the coarsest and highest abundances of siliciclastic sediments.

#### *Hanzawaia Biofacies*

Factor 1 (37% of the variance explained; Fig. 2) is characterized by the common occurrences of *Hanzawaia mauricensis*, *Cibicidina mississippiensis*, and *Spiroplectammina alabamaensis*. It is characteristic of the Cocoa Sand, the upper Red Bluff Formation, and upper Marianna Formation. The *Hanzawaia* biofacies represents deeper water than the *Nonion* biofacies based on lithologic and faunal (5% planktonic foraminifera) criteria. Modern *Hanzawaia* are typical of shelf environments (generally <100 m; Murray, 1991). In New Jersey, paleoslope modeling was used to estimate water depths of 75 ± 15 m for a middle Eocene *Hanzawaia mauricensis* biofacies (Olsson and Wise, 1987), and we infer similar depths for the *Hanzawaia* biofacies in Alabama.

#### *Siphonina-Cibicidoides Biofacies*

Factor 3 (11% of the variance explained; Fig. 2) is characterized by the common occurrences of *Cibicidoides cookei* and *Siphonina eocenica.* This biofacies is found in the Pachuta Marl, Mint Spring formation, basal Marianna Formation, and Bumpnose Formation. The *Siphonina-Cibicidoides* biofacies is indicative of water depths of ~100 m, based on paleoslope estimates for a similar biofacies in New Jersey (Olsson and Wise 1987).

#### *Uvigerina Biofacies*

Factor 4 (17% of the variance explained; Fig. 2) is characterized by the common occurrences of *Uvigerina byramensis* and *Uvigerina gardinerae*. This biofacies is found in the Shubuta Marl and the Bumpnose Formation. The *Uvigerina* biofacies contains 9% planktonic foraminifera and has an inferred water depth of ~125 m. *Bulimina jacksonensis*, a minor constituent of this biofacies, is typically found in modern outer neritic and deeper environments (van Morkhoven et al., 1986). In the modern oceans, *Uvigerina* generally occurs in outer neritic-bathyal (>100 m) environments and is often associated with low oxygen and/or organic-rich sediments (Miller and Lohmann 1982). *Uvigerina* is used frequently as a marker for the MFS (e.g., Loutit et al., 1988).

### SSQ Lithostratigraphy and Sequence Stratigraphy

There is general agreement about the identification of upper Eocene–Oligocene lithostratigraphic units in Alabama and Mississippi (Baum and Vail, 1988; Loutit et al., 1988; Tew, 1992), but there is disagreement as to their sequence stratigraphy, particularly the significance of stratal surfaces at the top of the Shubuta Marl of the Yazoo Formation and the top of the Glendon Limestone (Dockery, 1982; Baum and Vail, 1988; Tew, 1992; Miller et al., 1993; Jaramillo and Oboh-Ikuenobe, 1999; Echols et al., 2003). We based our identification of sequence on surfaces noted in the core, facies shifts, sharp changes in biofacies, and gamma log changes. The sequences in the SSQ core hole are similar to those in New Jersey: both generally have thin glauconite beds at the base representing the TST, and siliciclastic sediments at the top representing the regressive HST, although highstand sands are lacking from most of the SSQ sequences. Rapid shifts from shallow-water biofacies to deeper water biofacies are associated with sequence boundaries (Fig. 2). The pattern of deepening across sequence boundaries results from overstepping of facies due to the general absence of lowstand deposits in the coastal plain, as expected from sequence stratigraphic models (Posamentier et al., 1988). One exception to this appears to be the basal Bumpnose (see following). We assign sediments spanning the Eocene–Oligocene transition to seven sequences bracketed by sequence boundaries (Fig. 7): (1) the North Twistwood Creek–Cocoa Sand contact (chron C16n); (2) the mid-Pachuta Marl (mid-C13r–C15r); (3) the Shubuta-Bumpnose contact (latest chron C13r; the earliest Oligocene event); (4) the Mint Spring–Red Bluff contact (C13n-C12r boundary); (5) the Glendon-Byram contact (C12n-C11r); and

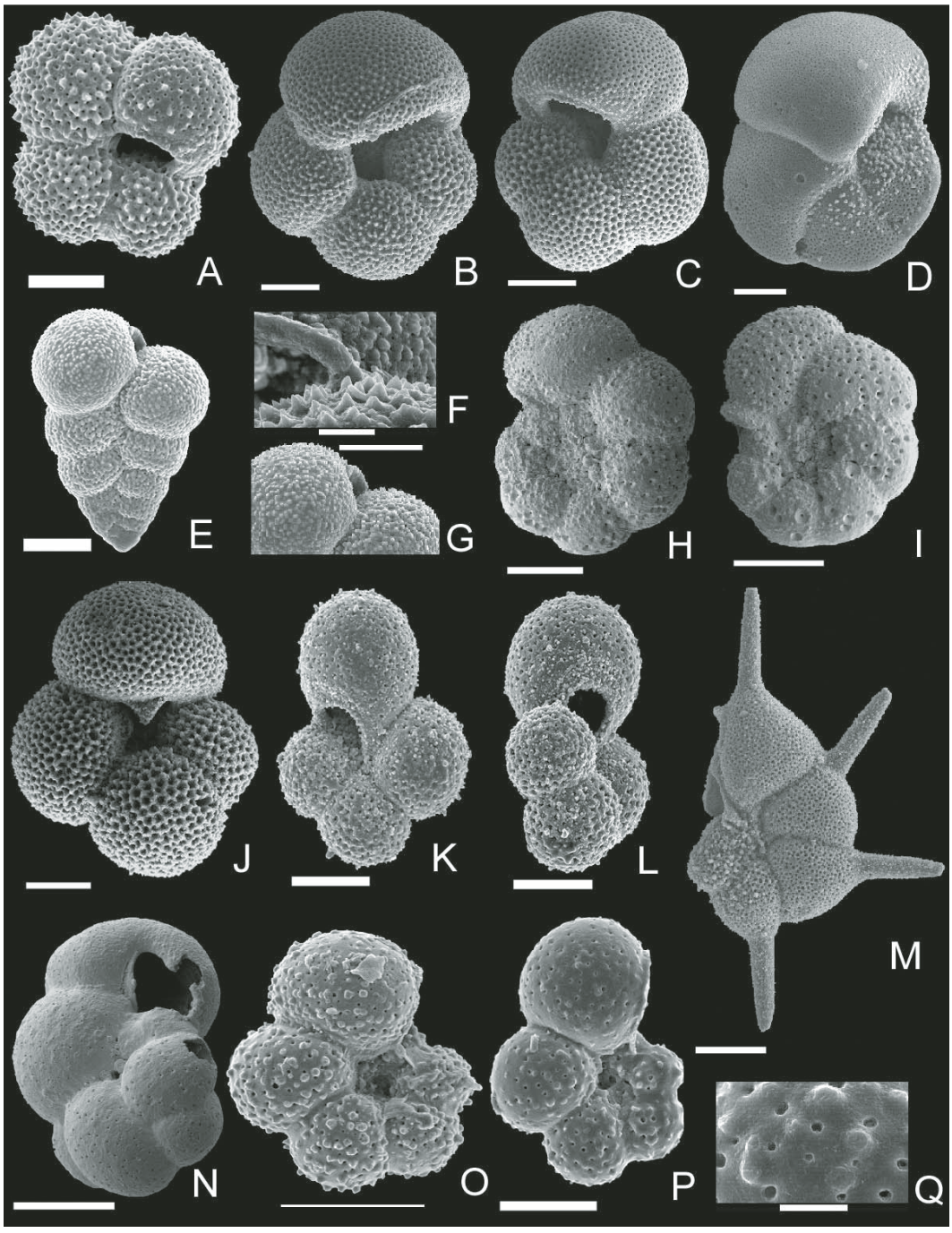


**Figure 6. Scanning electron microscope micrographs of planktonic foraminifera from St. Stephens Quarry. All scale bars 50 μm unless indicated. (A) *Globoturborotalia martini*, 152.1 ft (46.36 m), Zone O1. (B) *Turborotalia ampliapertura*, 158.6 ft (48.33 m), Zone E16. Scale bar = 100 μm. (C) *Turborotalia ampliapertura*, 165.2 ft (50.34 m), Zone E16. Scale bar = 100 μm. (D) *Turborotalia cocoaensis*, 165.2 ft (50.34 m), Zone E16. Scale bar = 100 μm. (E–G) *Chiloguembelina ototara*, 152.1 ft (46.36 m), Zone O1. (F) Scale bar = 20 μm. (G) Scale bar = 10 μm. (H, I) *Pseudohastigerina naguewichiensis*, 156.5 ft (47.70 m), Zone O1. (J) *Dentoglobigerina spp.*, 165.2 ft (50.34 m), Zone E16. Scale bar = 100 μm. (K, L) *Protentella* spp. (same specimen), 160.8 ft (49.01 m), Zone E16. (M) *Hantkenina primitiva*, 165.2 ft (50.34 m), Zone E16. Scale bar = 100 μm. (N) *Cassigerinella chipolensis*, 152.1 ft (46.36 m), Zone O1. (O) *Dipsidripella danvillensis*, 178.0 ft (54.25 m). (P, Q) *Dipsidripella davillensis*, 178.0 (54.25 m). Scale bar in Q = 10 μm.**

(6) the Bucatunna-Chickasawhay contact (late C11r; the mid-Oligocene fall). The sequence boundaries at the base of the upper Moodys Branch and the top of the Chickasawhay were not evaluated. Of the six sequence boundaries, four have clear (~0.5–1.0 m.y.) hiatuses associated with them (Fig. 3), and short hiatuses (<<0.5 m.y.) may be inferred for the other two (Fig. 4). Three of the sequence boundaries were recognized previously by Exxon (Fig. 1; e.g., Baum and Vail, 1988).

### *Upper Moodys Branch–North Twistwood Creek Sequence*

The lowest sequence examined consists of the upper Moodys Branch Formation (231.8–241.7 ft; 70.65–73.67 m) and the North Twistwood Creek Clay (177–231.8 ft; 53.95–70.65 m). The Moodys Branch Formation (which consists of the informal lower and upper Moodys Branch Formation; 231.8–247.0 ft; 70.65–75.29 m) consists of pale yellow (2.5Y8/2) quartz and carbonate sandy clayey silt with a few percent of glauconite in a thin bed (5 cm) at the base. The formation is well bioturbated with generally thin burrows (1 mm) and rare large (to 5 cm) burrows and scattered opaque heavy minerals, shells, and shell molds throughout. The formation is uniform except for a tan, laminated slightly silty clay from 239.7 to 241.7 ft (73.06–73.67 m). The base of the clay at 241.7 ft (73.67 m) is the contact between the upper and lower Moodys Branch Formation and is interpreted as sequence boundary (Baum and

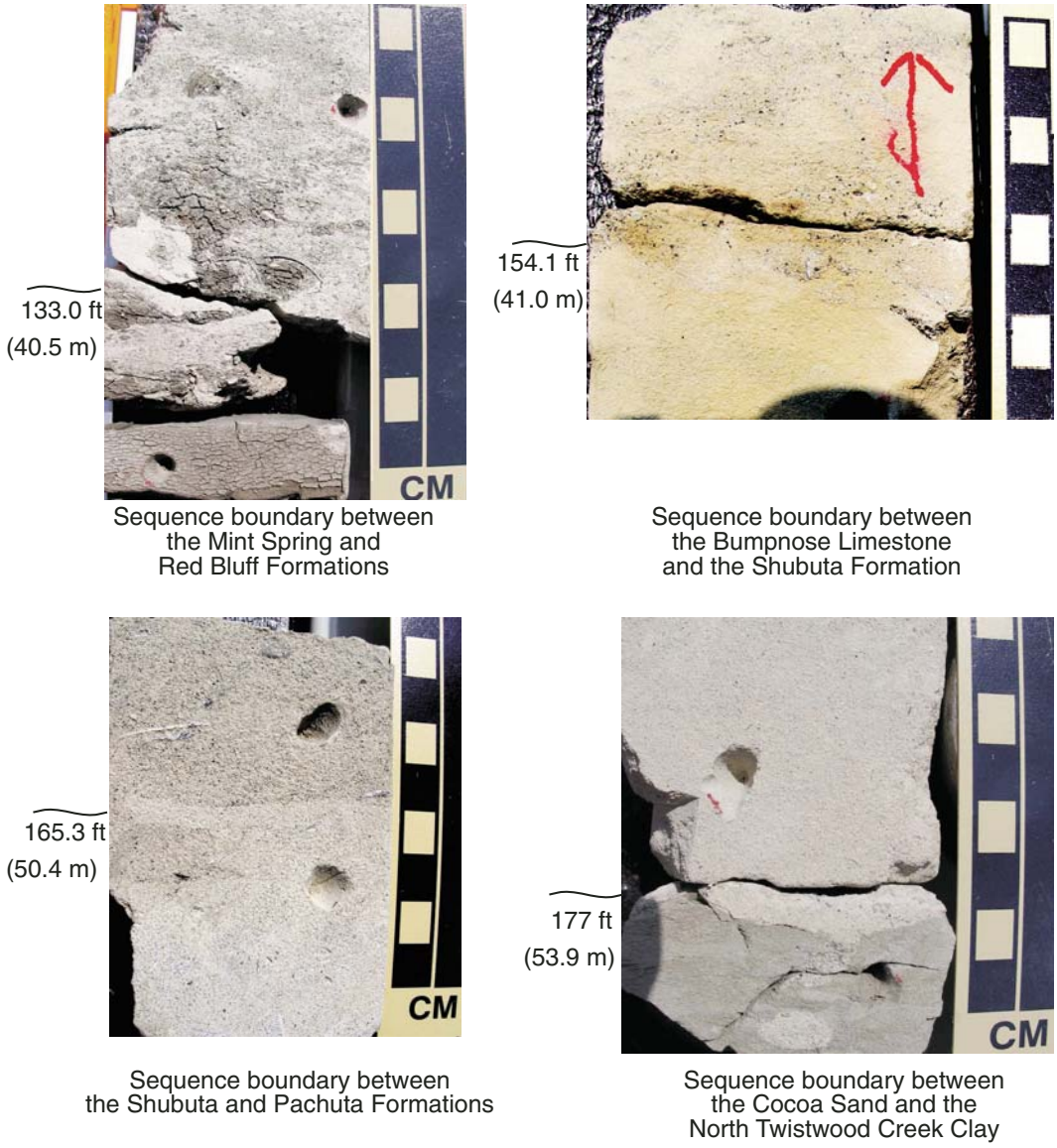


**Figure 7. Core photographs of sequence boundaries.**

Vail, 1988; P. Thompson, 1993, personal commun.). Our sample resolution is insufficient to further comment on this basal sequence boundary of the upper Moodys Branch–North Twistwood Creek sequence at 241.7 ft (73.67 m). The North Twistwood Creek Clay consists of light gray (2.5YR7/1), micaceous, slightly lignitic, quartzose sandy silt that becomes sandier upsection, with common fossils (thin shelled bivalves), laminations, and burrows that break many laminations. The upper Moodys Branch and North Twistwood Creek Formations are fine-grained sediments; the former contains more foraminifers, and glauconite and quartz sand increase upsection in the North Twistwood Creek Clay (Fig. 2). The upper Moodys Branch and North Twistwood Creek Clay are dominated by the *Nonion* biofacies (~30–50 m; Fig. 2). We tentatively place an MFS at 222 ft (67.67 m) at a major gamma peak, with values decreasing (coarsening) upsection above this. The contact of the North Twistwood Creek Formation (177.0 ft; 53.95 m) with the overlying Cocoa Formation is a distinct lithologic change and unconformity (Fig. 7), with an irregular surface associated with a gamma log increase (Fig. 4).

### *Cocoa–Lower Pachuta Sequence*

The Cocoa Member of the Yazoo Formation (172.2–177.0 ft; 52.49–53.95 m) is a sandy micrite and/or chalk in the core hole, with the percent sand never exceeding 50%. The sand-sized fraction is almost exclusively carbonate and composed largely of foraminifera. The carbonate in the mud fraction is presumably primarily nannofossils in these relatively deep water (>50 m) deposits, although a contribution by other carbonate mud sources cannot be precluded. The Cocoa Member is only slightly sandier than the Pachuta Member of the Yazoo Formation (159–172.2 ft; 48.46–52.49 m) and there is minimal lithologic difference between the Cocoa and the overlying Pachuta Member in the core hole. The lower part of the Pachuta Member consists of pale yellow (2.5Y8/2) sandy micrite with very little glauconite. It is differentiated from the upper part of the Pachuta Member above 165.3 ft (50.38 m), where glauconite is common. There is an irregular contact at 165.3 ft (50.38 m) within the mid-Pachuta with 0.1 ft (3 cm) of relief separating glauconitic micrite above and sandy micrite below (Fig. 7); the sand fraction below the surface has traces of quartz and little or no glauconite. This contact at 165.3 ft (50.38 m) is associated with a distinct gamma log increase (Fig. 4), and is interpreted as a sequence boundary associated

with a major hiatus (see Chronology section). The Cocoa–lower Pachuta sequence is the only sequence that lacks a distinct basal glauconitic interval. The MFS of the Cocoa–lower Pachuta sequence is tentatively placed at 174.5 ft (53.19 m), at a major gamma log peak. The Cocoa–lower Pachuta sequence was deposited in middle neritic environments (*Hanzawaia* biofacies; ~75 m water depth).

### *Upper Pachuta–Shubuta Sequence*

The upper part of the Pachuta Marl of the Yazoo Formation at SSQ consists of light gray (2.5Y7/2) slightly glauconitic to glauconitic sandy micrite, with glauconite generally decreasing upsection from the sequence boundary at 165.3 ft (50.38 m). Maximum water depths occur in a zone of maximum flooding from 163.7 to 157 ft (49.90–47.85 m) in a *Uvigerina* biofacies spanning the upper Pachuta to lower Shubuta members. The MFS is tentatively placed at 161 ft (49.07 m) in the upper part of the Pachuta, where *Uvigerina* reaches maximum abundance. The Shubuta Member of the Yazoo Formation (154.1–159 ft; 46.97–48.46 m) consists of a clean, uniform, cream-white (5Y8/1) marly micrite with virtually no sand and silt. A subtle but distinct erosional surface occurs at a lithologic contact at 154.1 ft (46.97 m) (Fig. 7). Above the surface is a glauconitic micrite and/or chalk assigned to the Bumpnose Formation. The Shubuta was deposited in middle-outer neritic environments, with a distinct, abrupt shallowing upsection from a *Uvigerina* biofacies (~120 m water depth) to a *Hanzawaia* biofacies (~75 m water depth) at the top (154.6 ft; 47.12 m). There is a sharp shift in biofacies across the Shubuta-Bumpnose contact from the shallower water *Hanzawaia* biofacies to the deeper water *Siphonina-Uvigerina* biofacies.

We follow Miller et al. (1993) in placing a sequence boundary at the Shubuta-Bumpnose contact. In contrast, others (Baum and Vail, 1988; Loutit et al., 1988; Pasley and Hazel, 1990; Mancini and Tew, 1991; Tew, 1992; Jaramillo and Oboh-Ikuenobe, 1999; Echols et al., 2003) have interpreted the Cocoa Sand through the Red Bluff Formation as a single sequence (Fig. 1), the Shubuta Marl and Bumpnose Formation being separated by an MFS. They interpreted the surface separating the two formations as a starvation surface caused by sediments being trapped onshore. However, we show that: (1) a benthic foraminiferal biofacies shift occurs abruptly across the 154.1 ft (46.97 m) contact; (2) the contact is an erosional surface (Fig. 7); and (3) the amount of glauconite increases 2 ft (60 cm) above the contact. The combination of an abrupt biofacies shift and increase in glauconite is typical of other sequence boundaries in Alabama and New Jersey. Thus, we interpret the Shubuta-Bumpnose contact as a sequence-bounding unconformity, not an MFS. This agrees with Dockery's (1982) observation of lowermost Oligocene channels incised into the top of the Shubuta Member in Mississippi that are filled with the Forest Hills Sand, a lateral correlative of the Red Bluff Formation. Part of the controversy in the interpretation of the Shubuta–Red Bluff contact as a sequence boundary probably derives from the fact that the upper Pachuta–Shubuta sequence is a deep-water *Uvigerina* biofacies, except for the abrupt shallowing at the top. Although the deep-water *Uvigerina* interval was noted in previous biofacies studies of the SSQ outcrop (Loutit et al., 1988), the abrupt shallowing was missed due to sampling limitations.

### *Bumpnose–Red Bluff Sequence*

The overlying lower Oligocene sequence consists of the Bumpnose and the Red Bluff Formations. The Bumpnose Formation in the SSQ core hole occurs from 140.2 to 154.1 ft (42.73–46.97 m), where it consists of a slightly marly, slightly glauconitic to glauconitic, light greenish-gray (5GY8/1) micrite and/or chalk. Distinctly glauconitic zones occur at 151.3–154.1, 149.0–149.6, and 146.6–147.0 ft (46.12–46.97 m, 45.42–45.60 m, and 44.68–44.81 m) and glauconite generally decreases upsection above this in the lower Bumpnose Formation, beginning at ~146 ft (44.50 m). An MFS associated with a peak abundance of *Uvigerina* could tentatively be placed at 152.1 ft (46.36 m); however, because common glauconite continues upsection to 149.0 ft (45.42 m) in the *Siphonina* biofacies, we place the MFS at this level, with a TST from 2 ft (60 cm) above the base of the sequence to 149.0 ft (45.42 m) (the lower 2 ft may be a lowstand systems tract [LST], as discussed in the following). A change to the shallower *Hanzawaia* biofacies above 147.5 ft (44.96 m) indicates the regressive HST. The Red Bluff Formation in the SSQ core hole occurs from 133.0 to 140.2 ft (40.54–42.73 m), where it consists of brown clay with scattered pyrite nodules (~15 cm spacing) that is siltier near the base. The formation was deposited in middle neritic (~75 m) water depths associated with the *Hanzawaia* biofacies. This is a typical sequence in that it contains glauconite near the base with carbonate-rich sediments above. The benthic *Uvigerina* biofacies indicates that the sequence is deepest near its base and progressively shallows upward.

### *Mint Spring–Marianna–Glendon Sequence*

The Mint Spring formation and Marianna and Glendon Formations comprise a thick (133.0–51 ft; 40.54–15.54 m) sequence at SSQ. The Mint Spring formation in the SSQ core hole occurs from 131.2 to 133.0 ft (39.99–40.54 m), where it consists of a glauconitic micrite and/or chalk. The base of the Mint Spring formation (133.0 ft; 40.54 m) is a sequence boundary consisting of a sharp, burrowed lithologic contact with rip-up clasts of the underlying brown clay and white (?kaolinite) clay clast and glauconite and shell concentrations at the base of the formation. There is a consensus that the contact at base of the Mint Spring formation is a sequence boundary (Baum and Vail, 1988; Mancini and Tew, 1991; Tew, 1992; Jaramillo and Oboh-Ikuenobe, 1999; Echols et al., 2003). The Mint Spring formation was deposited in middle-outer neritic environments (~100 m water depth) associated with the *Siphonina* biofacies.

The Marianna Formation in the SSQ core hole (59.5–131.2 ft; 18.14–39.99 m) is a heavily bioturbated, slightly marly, white (5Y8/1) micrite with scattered pyrite and opaque heavy minerals. The formation is generally friable, shows no evidence of cementation across grains, and is best termed a chalk in the diagenetic series ooze-chalk-limestone, except for a shelly limestone from 66.7 to 67.3 ft (20.33–20.51 m). The base of the Marianna Formation is placed at a change to a glauconitic micrite at 131.2 ft (39.99 m). We interpret this contact as the MFS of the Mint Spring–Marianna sequence; a mixed *Uvigerina-Siphonina* biofaces is associated with the MFS (~125 m water depth). Above this, the Marianna Formation shallows upsection from the *Siphonina* (~100 m water depth) to the *Hanzawaia* biofacies (~75 m water depth).

The interpretation of the Glendon Limestone (51–59.5 ft; 15.54–18.14 m) is problematic. This unit in the SSQ core hole is a limestone consisting of bluish-gray (10B5/1) to pale yellow (2.5Y8/3), heavily indurated, shell-rich micrite to micritic shell hash. Tew (1992) regarded the Glendon Limestone as the highstand deposit of the underlying sequence and placed a sequence boundary at its top. In contrast, Baum and Vail (1988) interpreted it as the lowstand deposits of the overlying sequence. The Glendon Limestone did not disaggregate and benthic foraminifers could not be separated. Thus, we cannot rely on foraminifera to place constraints on water-depth changes and placement of the sequence boundary. A major facies shift occurs at the top of the Glendon Formation in the core hole, associated with a large gamma log increase (Fig. 2), and we follow Tew (1992) in placing a sequence boundary at the top of the Glendon Formation. Integration of magnetobiostratigraphy indicates a significant hiatus (0.8–1.3 m.y.) between the Glendon and Byram Formations (Fig. 3; see Chronology section), further supporting our interpretation.

***Byram–Bucatunna Sequence***

The Byram–Bucatunna sequence consists of the Byram (undifferentiated) Formation (49–51 ft; 14.94–15.54 m) and Bucatunna Member (22.5–49 ft; 6.86–14.94 m). The basal sequence boundary is an abrupt contact at 51 ft (15.54 m) with the indurated Glendon Limestone below and a poorly sorted shell hash above. There is a very large gamma log increase associated with the contact (Fig. 2). The Byram Formation is a grayish-brown (10YR5/2) shelly silty clay and is more fossiliferous than the overlying Bucatunna Member, which is a grayish-brown micaceous, lignitic silty clay. This is a fine-grained sequence with a minor sand fraction dominated by the *Hanzawaia* biofacies. *Cibicidina* and *Astigerina subacuta* dominate a sample near the top of the Bucatunna Member. We interpret this as indicating shallowing upsection, although an MFS was not identified.

***Chickasawhay Sequence***

The Chickasawhay sequence (6.0–22.5 ft; 1.83–6.86 m) has a sharp basal sequence boundary with white (10YR8/1) partly indurated silty clayey foraminiferal quartz sand above and a grayish-brown micaceous, lignitic silty clay of the Bucatunna Member below associated with a sharp gamma log decrease (Fig. 2). The base of the Chickasawhay Formation is a major mid-Oligocene disconformity, the global correlation of which was discussed in detail by Miller et al. (1993). The top of the Chickasawhay Formation is heavily weathered between 6 and 10 ft (1.83–3.05 m). The depositional environment of the Chickasawhay Formation and sequence is middle neritic, based on qualitative examination of benthic foraminifera (foraminiferal recovery from the formation was insufficient for quantitative evaluation).

## Planktonic Foraminiferal Biostratigraphy

We examined 83 samples at SSQ from 75 to 230 ft (22.86–70.10 m) for planktonic foraminiferal biostratigraphic analysis. Planktonic foraminifera are extremely varied in terms of their abundance, diversity, and preservation. Samples range from full planktonic foraminiferal assemblages consistent with open ocean environments, to almost monospecific assemblages of tenuitellids and *Dipsidripella danvillensis*. Preservation of planktonic foraminifera appears to be facies dependent, and ranges from extremely well preserved, glassy specimens, to recrystallized (white) specimens.

Planktonic foraminiferal assemblages are dominated by dentoglobigerinids (*D. galavisi*, *D. pseudovenezuelana*, *D. tripartita*) and *Turborotalia ampliapertura*. The small size fractions (<125 µm) contain common *Pseudohastigerina* and tenuitellids. *Globigerinatheka* spp. were absent from all samples, and possibly excluded due to shallow water depths. Therefore, we were unable to constrain the highest occurrence (HO) of *G. index* at SSQ and the zone E15-E16 boundary.

The Eocene-Oligocene boundary is characterized by the extinction of family Hantkeninidae at 33.7 Ma in the global stratotype at Massignano, Italy (Premoli Silva and Jenkins, 1993; Berggren and Pearson, 2005; note that this level was assigned an astronomical age of 33.714 by Jovane et al., 2006). *Hantkenina* and *Cribrohantkenina* are extremely rare in the SSQ core hole, and we were not able to confidently place the Eocene-Oligocene boundary using the HO *Hantkenina*, which occurs in the core hole in the upper Pachuta Member at 163 ft (49.68 m) (see also Miller et al., 1993). Mancini (1979) reported the HO of *Hantkenina* spp. at the top of the Shubuta Member in outcrop at SSQ (equivalent to 154.1 ft [46.97 m] in the core hole). However, Bybell and Poore (1983) reported that specimens of *Hantkenina* in the upper Shubuta–Bumpnose are reworked based on analysis of nannofossils included in the foraminiferal tests, and Keller (1985) placed the HO of *Hantkenina* spp. in the basal Shubuta Member (equivalent to 158 ft (48.16 m) in the core hole, although there are uncertainties in core hole–outcrop correlations). The Eocene-Oligocene boundary is preceded by the extinction of the *Turborotalia cerroazulensis* group at 33.765 Ma (Berggren and Pearson, 2005). *Turborotalia* vary in abundance at SSQ; we find the HO of the *T. cerroazulensis* group at 162.0 ft (49.38 m), associated with the precursor $\delta^{18}O$ shift. Based on our age-depth plot anchored on the HO of *T. cerroazulensis* and the base of chronozone C13n, we predict that *Hantkenina* spp. should range to 157.5 ft (48.01 m) (lower Shubuta member), in agreement with Keller (1985).

*Cassigerinella chipolensis* (Fig. 6J) is rare. While the lowest occurrence (LO) of this species is not well calibrated to the time scale, the presence of *C. chipolensis* from 159 ft (48.46 m) at the base of the Shubuta Member suggests placement of the Eocene-Oligocene boundary (zone E16-O1) near this level (Miller et al., 1993).

The extinction of *Hantkenina* is also associated with the HO of *Pseudohastigerina* in the >125 µm size fraction (Nocchi et al., 1986). We find the HO of large *Pseudohastigerina* at 155.4 ft (47.37 m), approximating the top of planktonic foraminiferal biozone E16 (Berggren and Pearson, 2005) and the Eocene-Oligocene boundary.

This discussion highlights the problems in using biostratigraphic markers for very high resolution (~100 k.y.) correlations in nearshore sections. Although the Eocene-Oligocene boundary is firmly placed on chron C13n.12 at Massignano stratotype, it is not possible to interpolate the precise position of this chron at SSQ because two sequence boundaries occur within it and biostratigraphic criteria must be used. The Eocene-Oligocene boundary could be placed using biostratigraphic criteria at SSQ at 163 ft (HO of *Hantkenina*, which is certainly depressed at this location), 162 ft (49.38 m) (HO of *T. cerroazulensis* group, calibrated as ~65 k.y. older than the boundary; Berggren and Pearson, 2005), 159 ft (48.46 m; LO of *C. chipolensis*, poorly calibrated to time scale), 157.5 ft (48.01 m) (predicted HO of *Hantkenina* in the core hole and the HO of common, unreworked *Hantkenina* in the outcrop; Keller, 1985), or 155.5 (47.40 m; HO of large *Pseudohastigerina* spp.). This difference of 5.5 ft (1.68 m) only represents 140 k.y. based on the sedimentation rate of 12 m/m.y. (Fig. 4). Similarly, the uncertainty in the HO of *Hantkenina* due to reworking (i.e., reported to an equivalent position of 154.1 ft [46.97 m] in the outcrop versus 163 ft [49.68 m] observed and 157.5 ft [48.01 m] predicted) amounts to only 100–200 k.y. This uncertainly is reflected in the stairstep placement of the Eocene-Oligocene boundary (Fig. 4). We favor placing the boundary in the lower Shubuta Marl (157.5 ft) at the predicted HO of *Hantkenina*.

Insights into foraminiferal preservation can be gained from SSQ. Planktonic foraminifera preservation tracks sequence boundaries and better preservation is associated with intervals of higher clay content. Within the North Twistwood Creek Clay (177–231.8 ft; 53.95–70.65 m), foraminifera are rare but extremely well preserved (Figs. 6). Foraminifera from the Cocoa–lower Pachuta sequence (177–163.7 ft; 53.95–49.90 m) are recrystallized and appear white under the light microscope. From 163.7 to 150.2 ft (49.90–45.78 m), foraminifera from the Shubuta Marl and lower Bumpnose–Red Bluff sequence are glassy (Fig. 6), except for a thin interval of recrystallization from 156.5 to 154.1 ft (47.70–46.97 m). Preservation deteriorates and foraminifera are recrystallized from 150.2 to 140.2 ft (45.78–42.73 m), with glassy specimens from 140.2 to 131.2 ft (42.73–39.99 m).

## Nannofossil Biostratigraphy

The abundance and preservation of coccoliths and the diversity of their assemblages vary considerably in the section. There is a striking contrast between scarce to common, moderately to poorly (micritization) preserved assemblages between 271.1 and 166.8 ft (82.63–51.42 m; Moodys Branch to lower Pachuta) and the

abundant, high-diversity, well-preserved assemblages between 163 and 142 ft (49.68–43.28 m; upper Pachuta to Bumpnose). The lower part of the section (i.e., the lower Moodys Branch Formation) is well anchored by the occurrence of a diverse, typical Bartonian (zone NP17) assemblage at 269.5 ft (82.14 m) with *Campylosphaera dela* (HO in upper zone NP17), *Discoaster barbadiensis*, *D. saipanensis*, *Ericsonia formosa*, *Reticulofenestra reticulata*, *R. umbilicus*, and *Sphenolithus obtusus* (restricted to zone NP17). The interval between 268.8 and 206 ft (81.93–62.79 m; lower Moodys Branch through North Twistwood Creek Clay) comprises an alternation of levels with abundant and well-preserved coccoliths and micritic levels with rare, heavily recrystallized nannofossils. Even where preservation is best, this interval lacks biostratigraphic markers (e.g., *Chiasmolithus oamaruensis*, *Helicosphaera reticulata*, and *Isthmolithus recurvus*). It is assigned to zone NP18 because of the lowest occurrence (LO) of *Isthmolithus recurvus* at 178 ft (54.25 m; just below the North Twistwood Creek Clay–Cocoa Sand formational contact), which defines the base of zone NP19–20. The Cocoa–lower Pachuta sequence (176–166.8 ft; 53.64–50.84 m) yields very impoverished assemblages because of extremely poor preservation. However, *Reticulofenestra reticulata* and *Ericsonia formosa* occur consistently and abundantly through the sequence, with occasional, generally overgrown, rosette-shaped discoasters, including *D. barbadiensis* (at 168 ft; 51.21 m) and *D. saipanensis* (at 166.8 ft; 50.84 m). *Reticulofenestra reticulata* ranges from middle Eocene (upper zone NP16) up to a level within zone NP19–20, and can be used to subdivide that zone. Its common occurrence in the Cocoa–lower Pachuta sequence indicates zone NP19–20, and its HO at the unconformable sequence boundary at 165.3 ft (50.38 m) indicates that the zone is truncated. The upper Pachuta to Bumpnose succession (comprising the upper Pachuta–Shubuta and Bumpnose–Red Bluff partim sequences) up to 142 ft (43.28 m) yields abundant and well-preserved assemblages of zone NP21. In this interval, the fine fraction is mostly composed of coccoliths, with little or no detrital particles (in contrast to the underlying sediments). Preservation and calcareous nannofossil abundance decrease markedly above 144 ft (43.89 m). Zone NP21 extends up to 110.6 ft (33.71 m). The interval between 96 ft and 14 ft (29.26–4.27 m) belongs to zone NP 23.

## Chronology

In view of controversies surrounding the sequence stratigraphic framework at St. Stephens Quarry, Miller et al. (1993) conservatively estimated continuous sedimentation between magnetochron boundaries. We reevaluated the SSQ chronology of Miller et al. (1993) using new biostratigraphic data (Figs. 3 and 4) indicating that there are hiatuses at many sequence boundaries. Our age control varies from ±0.1 to ±0.5 m.y. based on integration of magnetobiostratigraphy; individual biostratigraphic datum levels typically have errors on the order of 0.5 m.y., but the identification of magnetochrons and integration with biostratigraphy improves age control to as fine as ±0.1 m.y. Our chronologic control is sufficient to generally constrain sedimentation rates as 13–24 m/m.y. within individual sequences, but is not sufficient to resolve detailed sedimentation rate changes within sequences as they coarsen (shallow) upsection above MFSs. We assume that sedimentation rates were otherwise constant within sequences between these control points (Figs. 3 and 4); although this is certainly not correct, it results in age uncertainties that are relatively minor (<0.5 m.y.)

Integration of the biostratigraphic data with magnetostratigraphy is essential for the temporal interpretation of sections and the determination of the duration of hiatuses at sequence boundaries (Aubry, 1995, 1998). Integration of planktonic biostratigraphy and magnetostratigraphy within a sequence stratigraphic framework allows quantification of hiatuses and identification of unrepresented magnetochrons. Age assignments derived from planktonic foraminifera and the calcareous nannofossils are generally consistent (Figs. 3 and 4), although nannoplankton provide finer resolution for this interval (Aubry, 1995, 1998). The magnetostratigraphic record at SSQ has been previously interpreted to be complete from chron C16r through chron C11n (Miller et al., 1993). This interpretation is not supported by biostratigraphy that reveals three previously undetected hiatuses at the basal upper Moodys Branch–North Twistwood Creek (36.7–?37.5 Ma; Fig. 3), Cocoa–lower Pachuta (35.4–35.9 Ma), and upper Pachuta–Shubuta (33.9–35.0 Ma) sequence boundaries (Fig. 4).

Nannofossil biostratigraphy indicates the concatenation of chronozones C13r and C15r and C16n1 and C16n2 (i.e., chrons C15n and C16n1r are not represented). A magnetozone from 206 to 239.5 ft (62.79–73.0 m) was interpreted as chron C16n (Miller et al., 1993). The chron C16n-C15r reversal is associated with mid-biochron NP19–20 (Berggren et al., 1995); thus, if this normal polarity interval represented chron C16n, it should belong to zone NP19–20. This is not the case; the base of the zone occurs at 178 ft (54.25 m). We reinterpret the interval from 183 to 222.5 ft (55.78 to 67.82 m) as chronozone C16r, which correlates with zone NP18, and place a 0.5 m.y. hiatus at the base of the Cocoa–lower Pachuta sequence (Figs. 3 and 4); two normal points within this interval (206 and 209.5 ft; 62.79–63.86 m) are interpreted as normally overprinted. As a result, the normal from 226 to 239.5 ft (68.88–73.0 m) is interpreted as chron C17, not C16 n1. The thin normal polarity magnetozone between 176 and 178 ft (53.64–54.25 m) was interpreted as chron C15n (Miller et al., 1993), which is associated with the upper part of zone NP19–20. This thin magnetozone is now interpreted as the concatenation of chrons C16n1 and C16n2. Chronozone C13r of Miller et al. (1993) is now interpreted as a concatenation of chrons C13r and C15r, with a hiatus longer than 1 m.y. (33.9–35.0 Ma) associated with the basal upper Pachuta–Shubuta sequence boundary.

Planktonic biostratigraphy support the interpretation of the identification of chronozones C13r through C11n (Fig. 3). The normal magnetozone between 133.8 and 151 ft (40.78–46.02 m; Bumpnose and Red Bluff) is associated with zone NP21 and can be confidently interpreted as chron C13n. The reversed polarity interval between 152.1 ft and 165.3 ft (50.38 m) represents the late part of chron C13r, and the upper surface of the sequence boundary at 165.3 ft (50.38 m) (lower Pachuta–upper Pachuta contact) is ca. 33.9 Ma. The interpretation of the normal polarity magnetozone between 50.8 and 50 ft (15.48–15.24 m) as chron C12n is compatible with the NP23 zonal and the P19 zonal assignment. However, we note the thinness of this interval and its proximity to the Glendon-Byram Formation contact, implying that only part of the chron is recorded. The age-depth diagram (Fig. 3) indicates that there is a >1 m.y. hiatus associated with this disconformity.

Integrating the calcareous biostratigraphy and magnetostratigraphy within the sequence stratigraphic framework, we propose a revised chronology for the stratigraphy in the SSQ core hole (Figs. 3 and 4). Using the age-depth diagrams, we derive ages for the sequences as follows.

1. The upper Moodys Branch–North Twistwood Creek sequence was deposited between 36.7 and 35.9 Ma (Fig. 3; chron C17n partim to C16n2 partim) (the lower Moodys Branch is part of an older sequence).

2. The Cocoa–lower Pachuta sequence was deposited from 35.4 to 35.0 Ma (Figs. 3 and 4). The hiatus across the 165.3 ft (50.38 m) sequence boundary is estimated as 35.0–33.9 Ma.

3. The upper Pachuta–Shubuta sequence spans the Eocene-Oligocene boundary as it is defined at Massignano as the level associated with the HO of *Hantkenina* spp. (Pomerol and Premoli Silva, 1988; Premoli Silva and Jenkins,

1993). Considerable controversy has attended the placement of this boundary at SSQ because of uncertainties in biostratigraphy, primarily due to reworking (see Planktonic Foraminiferal Biostratigraphy section). The upper Pachuta–Shubuta sequence is entirely in chronozone C13r (Figs. 3 and 4), and we prefer a placement of the Eocene-Oligocene boundary in the middle of the Shubuta at 157.5 ft (48.01 m) immediately above the first occurrence (FO) of *Cassigerinella chipolensis* at 158.0 ft (48.16 m) (see Planktonic Foraminiferal Biostratigraphy section). Our best estimate for the age of the sequence is ca. 33.9–33.6 Ma (i.e., using a sedimentation rate of 1.0 cm/k.y. between the *Turoborotalia cerroazulensis*, *C. chipolensis*, and chron C13n datum levels; Fig. 4).

4. The Bumpnose–Red Bluff sequence was deposited between 33.6 and 33.0 Ma (Figs. 3 and 4), consistent with its correlation to chronozone C13n and uppermost C13r. The hiatus associated with the basal sequence boundary of the Bumpnose–Red Bluff sequence (i.e., the Shubuta-Red Bluff contact) is not discernable, although it appears to be much less than 100 k.y. based on extrapolation of sedimentation rates (e.g., 33.59–33.62 Ma; Fig. 4).

5. The Mint Spring–Marianna–Glendon sequence was deposited between 33.0 and 31.7 Ma (Figs. 3 and 4), consistent with its being rapidly deposited (1.8 cm/k.y.) in chron C12r. The younger age limit is uncertain and is based on the assumption that the HO of *Pseudohastigerina* spp. is in situ and not reworked as suggested by Miller et al. (1993), but it must be older than ca. 31 Ma (i.e., it is in chron C12r). Chronozone C12r partim is found in the Glendon Limestone (Fig. 2), as is the underlying Marianna Formation (Miller et al., 1993), whereas chronozone C12n-11r is found in the overlying Byram-Bucatunna Formations, suggesting placement of a sequence boundary at the top of the Glendon Limestone (Fig. 3).

6. The Byram–Bucatunna sequence was deposited from 30.3 to 30.5 Ma (chrons C11r–latest C12; Fig. 3).

7. The base of the Chickasawhay Formation is a major disconformity (Fig. 3) that represents the major mid-Oligocene unconformity of Vail et al. (1977). This surface was dated precisely for the first time at SSQ by Miller et al. (1993) as late chron C11r (ca. 30.1 Ma) and correlated with the oxygen isotope increase associated with Oi2 (Miller et al., 1993).

### Stable Isotopes

An ~0.9 ‰ $\delta^{18}O$ increase is associated with the C13r-13n boundary immediately above the HO of Eocene microplankton, and thus can be confidently correlated to the global Oi1 isotopic increase and $\delta^{18}O$ maximum (Miller et al., 1991) using magnetobiostratigraphic criteria (Fig. 8). The $\delta^{18}O$ increase begins in the core hole in association with the Shubuta-Bumpnose contact, an erosional surface, and a biofacies shift (i.e., the increase occurs between 155.5 and 152 ft [47.39–46.32 m]; Fig. 4); it culminates with maximum $\delta^{18}O$ values in the lowermost Bumpnose Formation at 152 ft (46.32 m). This requires that the sequence boundary was eroded very early in the sea-level fall and that deposition resumed during the later stages of the fall. This lag interval represents ~50 k.y., using the best estimate of sedimentation rates (1.1 cm/k.y.) for this section. Although water depth appears to increase across the sequence boundary (75 m below to 100 m above), we lack faunal samples from the critical 2 ft (60 cm) immediately above the sequence boundary. This interval lacks glauconite and is interpreted as an LST deposited during a time when sea level was falling globally (Fig. 9); glauconite and planktonic foraminifera increase immediately above this section at 152 ft (46.32 m) at the time of the lowest global sea level (i.e., associated with peak $\delta^{18}O$ values), marking the turning point and the beginning of the TST (see Fig. 9 and Discussion).

Though it is clear that the increase from 154 to 152 ft (46.93–46.32 m) is in fact Oi1, the precise timing of the increase relative to magnetic reversal history is uncertain. The sample with maximum $\delta^{18}O$ values (i.e., the base of zone Oi1; Miller et al., 1991) occurs in reversely magnetized sediments immediately below the transition to chronozone C13n (Fig. 4). At Pacific Site 1218, the maximum $\delta^{18}O$ values occur in a section correlated to chron C13n based on correlations from the magnetostratigraphy at nearby Site 1219 using percent carbonate data (Pälike et al., 2005; Lanci et al., 2005). At Site 522, maximum $\delta^{18}O$ values measured by Zachos et al. (1996) occur in normally magnetized sediments at 133.13 m (Tauxe and Hartl, 1997), although there is a coring gap from this sample to 134.0 m that spans the upper part of the $\delta^{18}O$ increase and the polarity transition. Although it is clear that the $\delta^{18}O$ increase associated with Oi1 begins in latest chron C13r, it is not clear when the actual maximum value occurs, although it does appear to be closely associated with the polarity transition.

A precursor $\delta^{18}O$ increase of ~0.5‰ occurs within the middle of chron C13r (Fig. 4). The precursor $\delta^{18}O$ increase is associated with the HO of the *T. cerroazulensis* group at 162.0 ft (49.38 m) and is thus latest Eocene (zone E16). It correlates with a similar event at Pacific Site 1218 (Fig. 8; Coxall et al., 2005). A 0.5‰ increase is readily resolvable given that precision is 0.08‰ for $\delta^{18}O$ and that natural variability is generally ~0.1‰; the similar patterns observed both in the Pacific and at SSQ document that this is a real increase, and that it was geographically widespread.

We have sufficient isotope data across two MFS (161 ft [49.07 m] in the upper Pachuta–Shubuta sequence and 149 ft [45.42 m] in the Bumpnose–Red Bluff sequence) to evaluate their relationships to temperature and ice volume. The 149 ft (45.42 m) surface is associated with decreases in $\delta^{18}O$ values, which is unexpected because it implies warmer temperatures in the deepest water depths. However, comparison with deep Pacific Site 1218 (Fig. 8) suggests that these $\delta^{18}O$ decreases may be global and associated with decreases in ice volume and eustatic rises. As noted above, the placement of the MFS in the upper Pachuta–Shubuta sequence is uncertain, with a zone of maximum flooding from 163.7 to 157 ft (49.90–47.85 m); this zone is associated in part with the interval of minimal $\delta^{18}O$ values at 163 ft (49.68 m).

Latest Eocene–earliest Oligocene (approximately chron C13r) $\delta^{18}O$ values average –0.65‰ at SSQ, whereas values in early Oligocene chron C13n average –0.11‰. Equilibrium $\delta^{18}O$ values can be calculated by adjusting the *Cibicidoides* values to the Neogene calibration of 0.64‰ (Shackleton et al., 1984), yielding –0.01‰ and 0.53‰, or the Paleogene calibration of 0.27‰ (Katz et al., 2003), yielding –0.38‰ and 0.16‰. Studies of the modern and Eocene–Oligocene Gulf of Mexico suggest that the local $\delta^{18}O_{seawater}$ at ~100 m water depth was +1.0‰ due to excess evaporation over precipitation (Kobashi et al., 2004). Using the paleotemperature equation of Barrera and Savin (1999) and an enrichment of surface water $\delta^{18}O_{seawater}$ of +1.0‰ over mean ocean $\delta^{18}O_{seawater}$, the late Eocene water temperatures at SSQ were between 16.3 and 20.5 °C. The 16.3 and 20.5 °C range reflects the difference between the assumption of an ice-free world ($\delta^{18}O_{seawater} = -1.2$‰) and a fully glaciated modern world ($\delta^{18}O_{seawater} = -0.28$‰; Shackleton and Kennett, 1975), respectively. For the earliest Oligocene, there is evidence that ice volumes were 75%–100% of modern size (Zachos et al., 1996; Miller et al., 2005a, 2005b), indicating that water temperatures for SSQ were between 17 and 18 °C for this period. Late Eocene ice volume is less defined, although 17.5–19 °C is predicted, assuming an ice sheet of 1/3–2/3 of modern volume (Miller et al., 2005b). Considering a margin of error, these temperatures of ~17–19 °C are similar to the modern values for water depths of ~100 m in the northeast Gulf of Mexico, which are typically 18–20 °C, with a minor seasonal variation of ±1 °C (Levitus, 1982; Kobashi et al., 2004; Golubev and Hsueh,

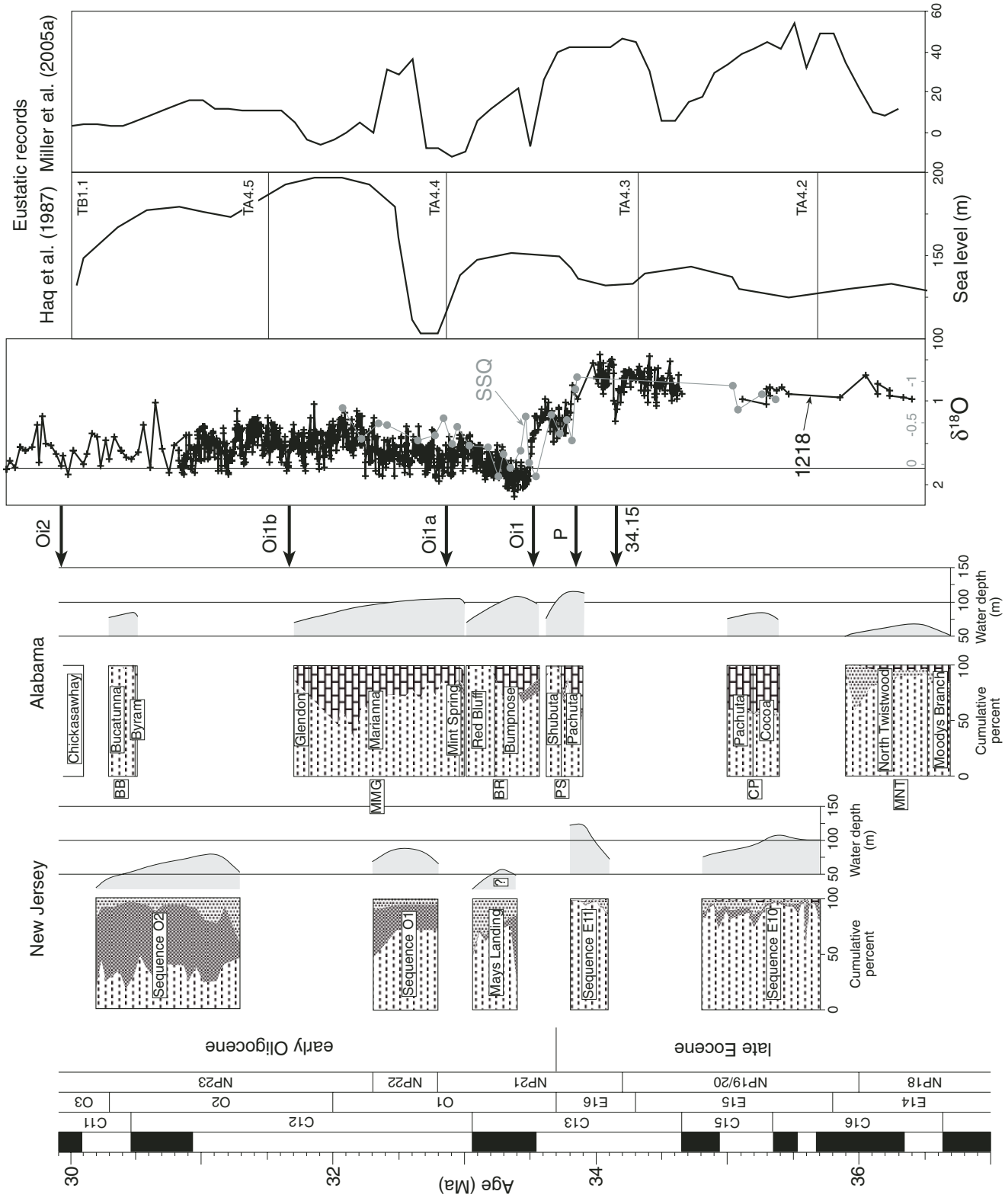


**Figure 8. Distribution of sediments from the upper Eocene–lower Oligocene of the New Jersey and Alabama coastal plains shown as a function of time and compared to the eustatic records of Miller et al. (2005a) and Haq et al. (1987; recalibrated to the time scale of Berggren et al., 1995 [BKSA, 95]) and the benthic foraminiferal $\delta^{18}O$ record at Site 1218 (Lear et al., 2004; Coxall et al., 2005) and SSQ (this study). P is precursor. Arrows are drawn isotopic maximum (e.g., Oi1, Oi1a). Lithology key is in Figure 2.**

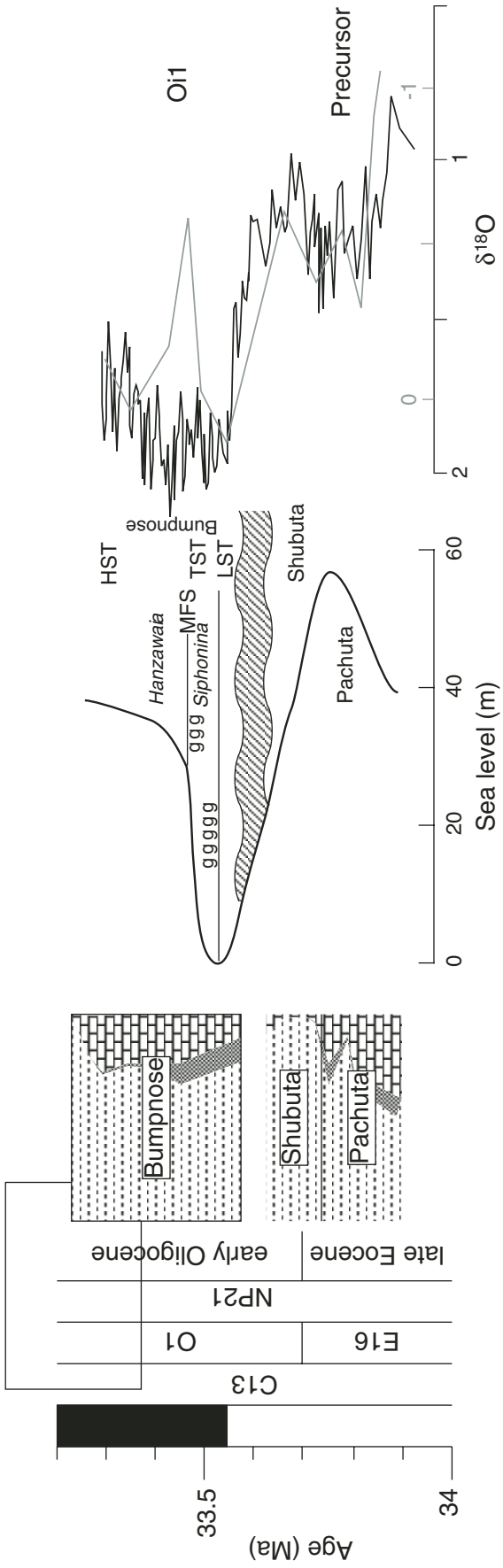


**Figure 9. Comparison of our eustatic model for the latest Eocene to earliest Oligocene (center panel) with the depositional history of the corresponding sequences. LST—lowstand system tract, TST—trangressive system, MFS—maximum flooding surface, HST—highstand systems tract, g—glauconite. On right are the oxygen isotopic records for Site 1218 (black) and SSQ (this study, red). Time scale of Berggren et al. (1995).**

2006). The ~1–3 °C cooler temperatures could be reconciled with modern temperatures by assuming that Eocene–Oligocene $\delta^{18}O_{seawater}$ in this region was ~0.5‰ higher than today (i.e., implying less Rayleigh fractionation on a planet with lower latitudinal thermal gradients than modern; Keigwin and Corliss, 1986) or could be simply attributed to uncertainties of ±2 °C in isotopic calibrations (e.g., near modern values are obtained using the Paleogene calibration).

The average SSQ $\delta^{18}O$ values of –0.65‰ (approximately chron C13r) and –0.11‰ (chron C13n) contrast with coeval Atlantic deep-sea $\delta^{18}O$ values in *Cibicidoides* of 0.8‰ before and 1.8‰ after Oi1 (Miller et al., 1987). Pacific values at Site 1218 are similar to those of the Atlantic (Fig. 8; Coxall et al., 2005), once adjusted for the 0.64‰ disequilibrium effects of *Cibicidoides* (Shackleton et al., 1984). The SSQ-Atlantic $\delta^{18}O$ differences of 1.5‰ and 1.9‰ for chron C13r and chron C13n, respectively, correspond to temperature differences of 6 and 8 °C, assuming that the shelf waters at SSQ were not significantly fractionated relative to the deep sea. With a +1.0‰ fractionation due to excess evaporation over precipitation (Kobashi et al., 2004), the temperature difference would be 10 and 12 °C, respectively. This vertical temperature difference is (1) less than the modern difference of ~17 °C, and (2) the ~2 °C increase in thermal gradient between the late Eocene and the early Oligocene reflects the development of a stronger vertical thermal gradient in the oceans at Oi1 time.

Carbon isotopic variations mimic $\delta^{18}O$ in chron C13 (Fig. 4). Such covariance across the Eocene-Oligocene transition was first noted by Zachos et al. (1996) and is explained by increased burial of organic carbon relative to carbonate carbon during the cooler intervals and/or those with greater ice volume. This covariance is consistent with the hypothesis that increasing latitudinal thermal gradients combined with decreasing deep ocean temperatures favored greater productivity levels by increasing wind-driven upwelling, which in turn provided more nutrients in the upper ocean that fueled increased primary and export production (Falkowski et al., 2004).

## DISCUSSION: COMPARISONS OF ALABAMA, NEW JERSEY, AND GLOBAL RECORDS

### Comparisons with New Jersey

Sequence boundaries in the New Jersey core holes were recognized using physical and geophysical criteria (including irregular contacts, reworking, bioturbation, major facies changes, and gamma ray peaks) and biofacies

changes (see summaries in Miller and Snyder, 1997). Five New Jersey sequences spanning the Eocene-Oligocene boundary, from oldest to youngest, were designated as E10, E11, ML, O1, and O2. Although these five sequences have not been found together in a single core hole, a composite chronology was constructed for the ACGS#4 (containing E10, E11, ML, and O1) and Island Beach (containing E10, E11, O1, and O2) core holes (Fig. 5), where the upper Eocene and lower Oligocene sequences are well preserved and well dated. Water depths were reconstructed using benthic foraminiferal and lithofacies constraints; foraminiferal constraints include comparison to fossil and modern benthic foraminiferal habitat studies and reconstruction of paleoslope models such as shown in Figure 2 for SSQ. Details of the depth assignments of the New Jersey Eocene and Oligocene biofacies were provided in Browning et al. (1997) and Pekar et al. (1997), respectively.

Although the coastal plains of Alabama and New Jersey are parts of passive margins with a similar time of rifting (Late Triassic–Early Jurassic), they differ in tectonic and sedimentation styles. Post-rift tectonics on the New Jersey coastal plain have been dominated by simple thermal and/or flexural subsidence and sediment loading (Watts and Steckler, 1979; Reynolds et al., 1991; Kominz et al., 1998; Van Sickel et al., 2004). Subsidence in the New Jersey coastal plain began ca. 120 Ma as the crust attained enough flexural rigidity to respond to thermal subsidence and loading by sediment offshore; the form of subsidence is that of a thermally subsiding basin (Watts, 1981). Detailed subsidence estimates obtained through backstripping of New Jersey coastal plain core holes documents that sediment loading dominated subsidence, that the residual subsidence can be fit to an exponential curve, and that there is no evidence for faulting or active tectonic subsidence (Kominz et al., 1998, 2002; Van Sickel et al., 2004). In general, onshore sedimentation rates have been low to modest (20 m/m.y.; Miller et al., 1998). This, together with low rates of tectonic subsidence by the late Eocene (<10 m/m.y.), indicates that the effects of tectonics and changes in sediment supply were subdued and the major influence on sedimentation is interpreted to have been sea-level change (Miller et al., 1998, 2005a). In contrast, the Gulf of Mexico underwent widespread salt tectonics, and evidence of faulting is more common than on the more passive margin of New Jersey. The SSQ core hole, for example, is on the flank of the Salt Mountain anticline. In addition, the depositional setting of the Alabama coastal plain is mixed siliciclastic and carbonate sediments versus primarily siliciclastic in New Jersey; therefore, the two regions are subject to different tectonic and sedimentation influences.

Despite their different settings, a comparison between the timing of the sequence boundaries found in New Jersey and Alabama matches remarkably well (Fig. 8). There are five sequences from 36 to 30 Ma in New Jersey and Alabama: (1) New Jersey sequence E10 corresponds with the Alabama Cocoa–lower Pachuta sequence; (2) New Jersey sequence E11 corresponds with the Alabama upper Pachuta–Shubuta sequence; (3) New Jersey sequence ML corresponds with the Alabama Bumpnose–Red Bluff sequence; (4) New Jersey sequence O1 corresponds with the Alabama Mint Spring–Marianna–Glendon sequence; and (5) New Jersey sequence O2 corresponds with the Alabama Byram–Bucatunna sequence. We interpret this close correspondence between the two records to indicate that sea-level change is the major control on sequence boundary formation on these two margins. The minor differences in the ages of preserved sequences between the regions reflect the influence of both tectonics and sedimentation on the two basins and minor discrepancies in the fine tuning of ages and correlating sequences.

Although the water depths inferred from the benthic foraminiferal biofacies at SSQ have not been backstripped and therefore cannot be considered a proxy for global sea level, the overall pattern of water depth changes is similar in the two basins. Late Eocene water depths in New Jersey were greater than or equal to those of Alabama (~75–100 m in sequence E10 versus ~50 m in the upper Moodys Branch–North Twistwood Creek sequence; ~75–125 m in both E11 and the Cocoa–lower Pachuta sequence). Lower Oligocene Alabama sequences are generally deeper water than those of New Jersey (<30 m in ML versus 75–100 in Bumpnose–Red Bluff; 75 m in O1 versus 75–100 in Mint Spring Marianna–Glendon sequence; and 50–57 m in O2 versus 75 m in Byram–Bucatunna). We emphasize that global trends are reflected in the water depth reconstructions from both regions and that regional differences in tectonics and sedimentation can account for the difference in magnitudes of changes.

## Oxygen Isotopes and Global Sea-Level Curves

We establish a first-order correlation between the Oi1 $\delta^{18}O$ increase and the basal sequence boundary of the Bumpnose–Red Bluff, linking glacioeustatic lowering and margin erosion (Fig. 4). We do not have sufficient isotopic resolution to test first-order links across other sequence boundaries, although we do show that at least one MFS is associated with lower $\delta^{18}O$ values (Fig. 4). The basal Bumpnose–Red Bluff sequence boundary is linked to the early part of a eustatic fall inferred from $\delta^{18}O$ (Fig. 4); in contrast, maximum $\delta^{18}O$ values of Oi1 occur above the sequence boundary in the Bumpnose, suggesting that the lowest eustatic lowstand was associated with resumption of deposition in the coastal plain. Although this may seem counterintuitive, Pitman (1978) first pointed out that continental margin erosion is most widespread at the time of the greatest rate of eustatic fall, not the lowest point of fall. Christie-Blick et al. (1990) demonstrated that the point of onlap, separating erosional from depositional settings, is equivalent to where the rate of sea-level fall is equal to the rate of subsidence; rapid downward shifts in onlap occur when the rate of fall is the greatest. In regions with slow subsidence, such as SSQ and New Jersey, the margin erosion can be widespread at the beginning of the eustatic fall (Christie-Blick and Driscoll, 1995), as observed here (Fig. 4).

The amplitude of the benthic foraminiferal Oi1 $\delta^{18}O$ increase at SSQ (~0.9‰) is similar to that at ODP Site 1218 (~1‰) in the deep-water Pacific (~1.0‰; Fig. 8); the total increase in the Pacific attains the full 1.5‰ amplitude cited by Tripati et al. (2005) only if the precursor increase is included. How much of the 0.9‰–1.0 ‰ increase at Oi1 is due to temperature and how much to ice volume? Kominz and Pekar (2001) and Miller et al. (2005a) provided a eustatic estimate of 55 m for the earliest Oligocene sea-level fall. This explains 0.55‰–0.6‰ of a global change in seawater $\delta^{18}O$ using the sea-level calibrations of 0.10‰/10 m indirectly derived for the Oligocene (Pekar et al., 2002), or the direct calibration of 0.11‰/10 m derived for the Pleistocene (Fairbanks and Matthews, 1978). This indicates that ~0.4‰–0.45‰ of the increase at Oi1 time was due to temperature, which requires an ~2 °C cooling.

A precursor $\delta^{18}O$ increase of 0.5‰ in midchron C13r at SSQ correlates with a similar increase at Pacific Site 1218 (Fig. 8). The lack of any significant sequence stratigraphic change at this level at SSQ suggests that this was primarily a cooling, not a sea-level or ice-volume event.

We illustrate the relationships between sea level and sequences (Fig. 9). A postulated sea-level curve was derived from the oxygen isotopic records, recognizing that the precursor increase is largely a temperature signal. The scaling of the sea-level fall (~50–60 m) is derived from backstripping in New Jersey. We show that the short hiatus and erosion occurred during the maximum rate of fall and that the lowermost part of the Bumpnose Formation was deposited as an LST.

The turnaround to rising sea level is associated with TST reflected by glauconitic sediments.

We show here that it is possible to obtain a first-order correlation between benthic foraminiferal $\delta^{18}O$ records and sequences in continental shelf settings. This has been done for continental slope sites (e.g., Site 904 Miocene record on the New Jersey slope; Miller and Snyder., 1997), but few studies have convincingly tied shallow shelf sequences and benthic foraminiferal $\delta^{18}O$ records. Baum et al. (1994) generated a bulk carbonate isotopic record at the Bay Minette, Alabama, core hole, and it is clear the bulk $\delta^{18}O$ can be used in stratigraphic correlations, but the bulk $\delta^{18}O$ signal is difficult to interpret in terms of global changes in temperature and ice volume.

Magnetobiostratigraphic and isotopic correlations spanning the Eocene-Oligocene transition have sufficient resolution (much better than 0.5 m.y.) to evaluate other links between sequences at SSQ and $\delta^{18}O$ increases at Pacific Site 1218 (Fig. 8). Sequence boundaries at the base of the Bumpnose–Red Bluff, Mint Spring–Marianna–Glendon, Byram–Bucatunna, and Chickasawhay sequences are correlated with global $\delta^{18}O$ increases associated with Oi1, Oi1a, Oi1b, and Oi2, respectively (Fig. 8). The sequence boundary at the base of the upper Pachuta–Shubuta sequence is associated with an unnamed $\delta^{18}O$ increase at Site 1218, with maximum values ca. 34.15 Ma (Fig. 8). There are insufficient isotopic and sequence stratigraphic data to evaluate a link to the basal Cocoa–lower Pachuta and upper Moodys Branch–North Twistwood Creek sequences. Thus, we link five of our seven sequence boundaries to late Eocene–mid-Oligocene $\delta^{18}O$ increases.

It has been established for some time that large, near modern-sized ice sheets existed in the icehouse world of the Oligocene and earlier (Miller et al., 1991, 2005b; Zachos et al., 1994). The presence of ice sheets in the Eocene and older Greenhouse world remains the subject of debate (see Miller et al., 2005a, 2005b). Our comparisons firmly link late Eocene sequence boundaries and glacioeustasy, demonstrating that large ice sheets existed during the late Eocene. For example, the unnamed $\delta^{18}O$ increase at 34.15 Ma is ~0.6‰ and is associated with a eustatic lowering of 40 m (Fig. 8; Miller et al., 2005a); this implies that an ice sheet of ~60% of the modern East Antarctic ice sheet developed at this time and that the deep sea cooled by ~1 °C.

Studies at Exxon (Vail et al., 1977; Haq et al., 1987) have provided estimates of eustatic change. The sequence boundaries at the bases of TA4.2, TA4.3, TA4.4, TA4.5, and TB1.1 (Haq et al., 1987) correspond to sequence boundaries found in New Jersey (bases of sequences E10, E11, O1, O2, and O3, respectively) and Alabama (bases of sequences Cocoa–lower Pachuta, upper Pachuta–Shubuta, Mint Spring–Marianna–Glendon, Byram–Bucatunna, and Chickasawhay, respectively; Fig. 8). The major difference in timing between the two records is that Haq et al. (1987) did not recognize a sequence boundary equivalent to the one at the base of the Oligocene (basal Bumpnose–Red Bluff sequence). In addition, sea-level amplitudes estimated by Haq et al. (1987) have been shown to be too high by a factor of 2–3 (cf. eustatic records of Haq et al. [1987] and Miller et al. [2005a] in Fig. 8).

Comparison of the SSQ core hole with the eustatic estimate derived from onshore New Jersey backstripping (Van Sickel et al., 2004; Miller et al., 2005a) both validates the estimate and shows the limitations of deriving a eustatic estimate in one region. Sequence boundaries at the bases of the Cocoa–lower Pachuta, upper Pachuta–Shubuta, Bumpnose–Red Bluff, Mint Spring–Marianna–Glendon, Byram–Bucatunna, and Chickasawhay sequences are associated with falls in the Miller et al. (2005a) eustatic curve. The amplitudes of the water depth changes of 50–100 m are consistent with the eustatic amplitudes, even though they have not been backstripped; the main effect on a slowly subsiding margin with a thin section like SSQ should be water depth loading, which should reduce the amplitudes to ~35–60 m, similar to the eustatic curve. However, the timing of the top of the Mint Spring–Marianna–Glendon sequence does not fit the New Jersey eustatic record (i.e., predicted to be ca. 35.8 versus 36.4 Ma), because it continues into the hiatus of New Jersey sequence O1 (Fig. 8). It is unclear which, if either, record reflects the true global sea-level change in these intervals of discrepancy; however, given that SSQ appears more complete than New Jersey, it is probably a better representation for the early Oligocene, and the eustatic record should be adjusted accordingly.

## CONCLUSIONS

Comparison of upper Eocene–lower Oligocene sequences in Alabama and New Jersey fulfills the first expectation of sequence stratigraphy: sequences are formed at the same time in basins that are geographically separated and subject to different tectonic and sedimentary regimes. We show that these sequence boundaries correlate with global $\delta^{18}O$ increases, suggesting that ice-volume changes and attendant rapid sea-level falls have been the primary agent responsible for forming sequence boundaries since the late Eocene. Both basins show a similar pattern after the sequence boundaries were formed: deposition resumed about the same time as the lowest glacioeustatic lowstands. Our data confirm previous models that suggest that formation of sequence boundaries is most sensitive not to the absolute position of sea level, but to the rate of change of sea level. SSQ provides a direct calibration between sea level and stable isotopic records and places constraints on the amount of temperature versus ice volume recorded in deep-sea $\delta^{18}O$ changes: the earliest Oligocene (35.7–33.5 Ma) Oi1 $\delta^{18}O$ increase was globally ~1.0‰; ~60% of this was due to a glacioeustatic lowering of 55 m and ~40% was due to a cooling of 2 °C. In contrast, a precursor (33.8 Ma) $\delta^{18}O$ increase of 0.5‰ can be attributed primarily to cooling. Ice volume controlled the development of sequence boundaries not only in the Oligocene icehouse, but also in the late Eocene greenhouse.

### ACKNOWLEDGMENTS

We thank ARCO and G. Baum for the insight to conduct continuous coring in the Alabama coastal plain. The National Science Foundation and New Jersey Geological Survey supported New Jersey drilling, and the U.S. Geological Survey drilled the New Jersey core holes. We thank D.V. Kent, C. Liu, R. Olsson, S. Pekar, and P. Sugarman for discussions and help in collecting the data, G. Baum for supplying samples, and W.A. Berggren, W.B. Harris, and an anonymous reviewer for reviews. This study was supported by National Science Foundation grants EAR-94-17108, EAR-03-07112, EAR-05-06720, and OCE-06-23256.

### REFERENCES CITED

Aubry, M.-P., 1992, Late Paleogene calcareous nannoplankton evolution: A tale of climatic deterioration, *in* Prothero, D., and Berggren, W.A., eds., The Eocene-Oligocene climatic and biotic changes: Princeton, New Jersey, Princeton University Press, p. 272–309.

Aubry, M.-P., 1995, From chronology to stratigraphy: Interpreting the stratigraphic record, *in* Berggren, W.A., et al., eds., Geochronology, time scales and global stratigraphic correlations: A unified temporal framework for an historical geology: SEPM (Society for Sedimentary Geology) Special Publication 54, p. 213–274.

Aubry, M.-P., 1998, Stratigraphic (dis)continuity and temporal resolution in the upper Paleocene–lower Eocene deep sea record, *in* Aubry, M.-P., et al., eds., Late Paleocene–early Eocene climatic and biotic events in the marine and terrestrial records: New York, Columbia University Press, p. 37–66.

Bandy, O.L., 1949, Eocene and Oligocene foraminifera from Little Stave Creek, Clarke County, Alabama: Bulletins of American Paleontology, v. 32, p. 1–211.

Barrera, E., and Savin, S.M., 1999, Evolution of late Campanian–Maastrichtian marine climates and oceans, *in* Barrera, E., and Johnson, C.C., eds., Evolution of the Cretaceous ocean-climate system: Geological Society of America Special Paper 332, p. 245–282.

Baum, G.R., and Vail, P.R., 1988, Sequence stratigraphic concepts applied to Paleogene outcrops, Gulf and Atlantic basins, *in* Wilgus, C.K., et al., eds., Sea level changes: An integrated approach: Society of Economic Paleontologists and Mineralogists Special Publication 42, p. 309–327.

Baum, J.S., Baum, G.R., Thompson, P.R., and Humphrey, J.D., 1994, Stable isotopic evidence for relative eustatic sea-level changes in Eocene to Oligocene carbonates,

Baldwin County, Alabama: Geological Society of America Bulletin, v. 106, p. 824–939, doi: 10.1130/0016-7606(1994)106<0824:SIEFRA>2.3.CO;2.

Benson, R., 1975, The origin of the psychrosphere as recorded in changes of deep-sea ostracode assemblages: Lethaia, v. 8, p. 69–83.

Berggren, W.A., and Pearson, P.N., 2005, A revised tropical to subtropical Paleogene planktonic foraminiferal zonation: Journal of Foraminiferal Research, v. 35, p. 279–298, doi: 10.2113/35.4.279.

Berggren, W.A., Kent, D.V., Swisher, C.C., and Aubry, M.-P., 1995, A revised Cenozoic geochronology and chronostratigraphy, *in* Berggren, W.A., et al., eds., Geochronology, time scales and global stratigraphic correlations: A unified temporal framework for an historical geology: SEPM (Society for Sedimentary Geology) Special Publication 54, p. 129–212.

Boersma, A., 1984, Handbook of common Tertiary *Uvigerina*: Stony Point, New York, Microclimates Press, 207 p.

Browning, J.V., Miller, K.G., and Bybell, L.M., 1997, Upper Eocene sequence stratigraphy and the Absecon Inlet Formation, New Jersey coastal plain, *in* Miller, K.G., and Snyder, S.W., Proceedings of the Ocean Drilling Program, Scientific results, Volume 150X: College Station, Texas, Ocean Drilling Program, p. 243–266.

Bybell, L.M., and Poore, R.Z., 1983, Reworked *Hantkenina* specimens at Little Stave Creek, Alabama: Gulf Coast Association of Geological Societies Transactions, v. 33, p. 253–256.

Charletta, A.C., 1980, Eocene benthic foraminiferal paleoecology and paleobathymetry of the New Jersey continental margin [Ph.D. thesis]: New Brunswick, New Jersey, Rutgers University, 84 p.

Christie-Blick, N., and Driscoll, N.W., 1995, Sequence stratigraphy: Annual Review of Earth and Planetary Sciences, v. 23, p. 451–478, doi: 10.1146/annurev.ea.23.050195.002315.

Christie-Blick, N., Mountain, G.S., and Miller, K.G., 1990, Seismic stratigraphic record of sea level change, *in* National Research Council, ed., Sea-level change: National Academy of Sciences Studies in Geophysics: Washington, D.C., National Academy Press, p. 116–140.

Corliss, B.H., Aubry, M.-P., Berggren, W.A., Fenner, J.M., Keigwin, L.D., and Keller, G., 1984, The Eocene/Oligocene boundary event in the deep sea: Science, v. 226, p. 806–810, doi: 10.1126/science.226.4676.806.

Coxall, H.K., Wilson, P.A., Pälike, H., Lear, C.H., and Backman, J., 2005, Rapid stepwise onset of Antarctic glaciation and deeper calcite compensation in the Pacific Ocean: Nature, v. 433, p. 53–57, doi: 10.1038/nature03135.

Dockery, D.T., III, 1982, Lower Oligocene bivalvia of the Vicksburg group in Mississippi: Mississippi Department of Natural Resources Bureau Geological Bulletin, v. 123, p. 1–261.

Douglas, R.G., 1979, Benthic foraminiferal ecology and paleoecology: A review of concepts and methods, *in* Lipps, J.H., et al., eds., Foraminiferal ecology and paleoecology: Society of Economic Paleontologists and Mineralogists Short Course no. 6, p. 21–53.

Echols, R.J., Armentrout, J.M., Root, S.A., Fearn, L.B., Cooke, J.C., Rodgers, B.K., and Thompson, P.R., 2003, Sequence stratigraphy of the Eocene/Oligocene boundary interval: Southeastern Mississippi, *in* Prothero, D.R., et al., eds., From greenhouse to icehouse: The marine Eocene-Oligocene transition: New York, Columbia University Press, p. 189–222.

Enright, R., 1969, The stratigraphy, micropaleontology, and paleoenvironmental analysis of the Eocene sediments of the New Jersey Coastal Plain [Ph.D. thesis]: New Brunswick, New Jersey, Rutgers University, 242 p.

Fairbanks, R.G., and Matthews, R.K., 1978, The oxygen isotope stratigraphy of the Pleistocene reef tracts of Barbados: West Indies: Quaternary Research, v. 10, p. 181–196.

Falkowski, P.G., Katz, M.E., Knoll, A., Quigg, A., Raven, J.A., Schofield, O., and Taylor, M., 2004, The evolutionary history of eukaryotic phytoplankton: Science, v. 305, p. 354–360, doi: 10.1126/science.1095964.

Golubev, Y., and Hsueh, Y., 2006, Temperature variability in the northeastern Gulf of Mexico in 1997–1998, ocean.fsu.edu/~hsueh/mms/coldevent_insert.doc.

Haq, B.U., Hardenbol, J., and Vail, P.R., 1987, Chronology of fluctuating sea levels since the Triassic (250 million years ago to present): Science, v. 235, p. 1156–1167, doi: 10.1126/science.235.4793.1156.

Hooker, J.J., Collinson, M.E., and Siller, N.P., 2004, Eocene-Oligocene mammalian faunal turnover in the Hampshire Basin, UK: Calibration to the global time scale and the major cooling event: Geological Society [London] Journal, v. 161, p. 161–172.

Jaramillo, C.A., and Oboh-Ikuenobe, F.E., 1999, Sequence stratigraphic interpretations from palynofacies, dinocyst and lithological data of upper Eocene–lower Oligocene strata in southern Mississippi and Alabama, U.S. Gulf Coast: Palaeogeography, Palaeoclimatology, Palaeoecology, v. 145, p. 259–302, doi: 10.1016/S0031-0182(98)00126-6.

Jones, G.D., 1983, Foraminiferal biostratigraphy and depositional history of the Middle Eocene rocks of the coastal plain of North Carolina: North Carolina Department of Natural Resources and Community Development, Division of Land Resources, Geological Survey, Section 8, Special Publication, 80 p.

Jovane, L., Florindo, F., Sprovieri, M., and Pälike, H., 2006, Astronomic calibration of the late Eocene/early Oligocene Massignano section (central Italy): Geochemistry, Geophysics, Geosystems, v. 7, p. Q07012, doi: 10.1029/2005GC001195.

Katz, M.E., Wright, J.D., Katz, D.R., Miller, K.G., Pak, D.K., Shackleton, N.J., and Thomas, E., 2003, Paleocene-Eocene benthic foraminiferal isotopes: Species reliability and interspecies correction factors: Paleoceanography, v. 18, p. 1024, doi: 10.1029/2002PA000798.

Keigwin, L.D., 1980, Paleoceanographic change in the Pacific at the Eocene-Oligocene boundary: Nature, v. 287, p. 722–725, doi: 10.1038/287722a0.

Keigwin, L.D., and Corliss, B.H., 1986, Stable isotopes in late middle Eocene to Oligocene foraminifera: Geological Society of America Bulletin, v. 97, p. 335–345, doi: 10.1130/0016-7606(1986)97<335:SIILME>2.0.CO;2.

Keller, G., 1985, Eocene and Oligocene stratigraphy and erosional unconformities in the Gulf of Mexico and Gulf Coast: Journal of Paleontology, v. 39, p. 882–903.

Kennett, J.P., and Shackleton, N.J., 1976, Oxygen isotope evidence for the development of the psychrosphere 38 Myr ago: Nature, v. 260, p. 513–515, doi: 10.1038/260513a0.

Kobashi, T., Grossman, E.L., Dockery, D.T., and Ivany, L.C., 2004, Water mass stablility reconstructions from greenhouse (Eocene) to icehouse (Oligocene) for the northern Gulf Coast continental shelf (USA): Paleoceanography, v. 19, PA1022, doi: 10.1029/2003PA000934.

Kominz, M.A., and Pekar, S.F., 2001, Oligocene eustasy from two-dimensional sequence stratigraphic backstripping: Geological Society of America Bulletin, v. 113, p. 291–304, doi: 10.1130/0016-7606(2001)113<0291:OEFTDS>2.0.CO;2.

Kominz, M.A., Miller, K.G., and Browning, J.V., 1998, Long-term and short-term global Cenozoic sea-level estimates: Geology, v. 26, p. 311–314, doi: 10.1130/0091-7613(1998)026<0311:LTASTG>2.3.CO;2.

Kominz, M.A., Van Sickel, W.A., Miller, K.G., and Browning, J.V., 2002, Sea-level estimates for the latest 100 million years: One-dimensional backstripping of onshore New Jersey boreholes, *in* Sequence stratigraphic models for exploration and production: Evolving methodology, emerging models and application case histories: 22nd Annual GCSSEPM Foundation Bob F. Perkins Research Conference, Proceedings, p. 303–315.

Lanci, L., Parés, J.M., Channell, J.E.T., and Kent, D.V., 2005, Oligocene magnetostratigraphy from equatorial Pacific sediments (ODP Sites 1218 and 1219, Leg 199): Earth and Planetary Science Letters, v. 237, p. 617–634, doi: 10.1016/j.epsl.2005.07.004.

Lear, C.H., Elderfield, H., and Wilson, P.A., 2000, Cenozoic deep-sea temperatures and global ice volumes from Mg/Ca in benthic foraminiferal calcite: Science, v. 287, p. 269–272, doi: 10.1126/science.287.5451.269.

Lear, C.H., Rosenthal, Y., Coxall, H.K., and Wilson, P.A., 2004, Late Eocene to early Miocene ice-sheet dynamics and the global carbon cycle: Paleoceanography, v. 19, p. PA4015, doi: 10.1029/2004PA001039.

Levitus, S., 1982, Climatological atlas of the world ocean: Washington, D.C., National Oceanographic and Atmospheric Administration Professional Paper 13, 173 p.

Loutit, T.S., Hardenbol, J., Vail, P.R., and Baum, G.R., 1988, Condensed section: The key to age determination and correlation of continental margin sequences, *in* Wilgus, C.K., et al., eds., Sea level changes: An integrated approach: Society of Economic Paleontologists and Mineralogists Special Publication 42, p. 183–213.

Mancini, E.A., 1979, Eocene-Oligocene boundary in southwest Alabama: Gulf Coast Association of Geological Societies Transactions, v. 29, p. 282–286.

Mancini, E.A., and Tew, B.H., 1991, Relationships of Paleogene stages and planktonic foraminiferal zone boundaries to lithostratigraphic and allostratigraphic contacts in the eastern Gulf Coastal Plain: Journal of Foraminiferal Research, v. 21, p. 48–66.

Martini, E., 1971, Standard Tertiary and Quaternary calcareous nannoplankton zonation, *in* Farinacci, A., ed., Proceedings of the Second International Conference on Planktonic Microfossils 1970: Rome, Edizioni Tecnoscienza, 2, p. 739–785.

Miller, K.G., 1992, Middle Eocene to Oligocene stable isotopes, climate, and deep-water history: The Terminal Eocene event?, *in* Prothero, D., and Berggren, W.A., eds., Eocene-Oligocene climatic and biotic evolution: Princeton, New Jersey, Princeton University Press, p. 160–177.

Miller, K.G., and Curry, W.B., 1982, Eocene to Oligocene benthic foraminiferal isotopic record in the Bay of Biscay: Nature, v. 296, p. 347–350, doi: 10.1038/296347a0.

Miller, K.G., and Lohmann, G.P., 1982, Environmental distribution of Recent benthic foraminifera on the northeast U.S. continental slope: Geological Society of America Bulletin, v. 93, p. 200–206, doi: 10.1130/0016-7606(1982)93<200:EDORBF>2.0.CO;2.

Miller, K.G., Fairbanks, R.G., and Mountain, G.S., 1987, Tertiary oxygen isotope synthesis, sea level history, and continental margin erosion: Paleoceanography, v. 2, p. 1–19.

Miller, K.G., Kent, D.V., Brower, A.N., Bybell, L., Feigenson, M.D., Olsson, R.K., and Poore, R.Z., 1990, Eocene-Oligocene sea-level changes on the New Jersey coastal plain linked to the deep-sea record: Geological Society of America Bulletin, v. 102, p. 331–339, doi: 10.1130/0016-7606(1990)102<0331:EOSLCO>2.3.CO;2.

Miller, K.G., Wright, J.D., and Fairbanks, R.G., 1991, Unlocking the ice house: Oligocene-Miocene oxygen isotopes, eustasy, and margin erosion: Journal of Geophysical Research, v. 96, p. 6829–6848.

Miller, K.G., Katz, M.E., and Berggren, W.A., 1992, Cenozoic deep-sea benthic foraminifera: A tale of three turnovers, *in* Takayanagi, Y., and Saito, T., eds., Studies in benthic foraminifera: Proceedings of the Fourth International Symposium on Benthic Foraminifera (Benthos '90): Sendai, Japan, Tokai University Press, p. 67–75.

Miller, K.G., Thompson, P.R., and Kent, D.V., 1993, Integrated stratigraphy of the Alabama coastal plain: Relationship of upper Eocene to Oligocene unconformities to glacioeustatic change: Paleoceanography, v. 8, p. 313–331.

Miller, K.G., and the Leg 150 Shipboard Party, 1994, Initial reports of the Ocean Drilling Program, Leg 150: College Station, Texas, Ocean Drilling Program, v. 150X, 59 p.

Miller, K.G., Mountain, G.S., the Leg 150 Shipboard Party, and Members of the New Jersey Coastal Plain Drilling Project, 1996, Drilling and dating New Jersey Oligocene-Miocene sequences: Ice volume, global sea level, and Exxon records: Science, v. 271, p. 1092–1094.

Miller, K.G., and Snyder, S.W., 1997, Proceedings of the Ocean Drilling Program, Scientific results, Volume 150X: College Station, Texas, Ocean Drilling Program, 388 p.

Miller, K.G., Mountain, G.S., Browning, J.V., Kominz, M., Sugarman, P.J., Christie-Blick, N., Katz, M.E., and Wright, J.D., 1998, Cenozoic global sea-level, sequences, and the New Jersey Transect: Results from coastal plain and slope drilling: Reviews of Geophysics, v. 36, p. 569–601, doi: 10.1029/98RG01624.

Miller, K.G., Kominz, M.A., Browning, J.V., Wright, J.D., Mountain, G.S., Katz, M.E., Sugarman, P.J., Cramer, B.S., Christie-Blick, N., and Pekar, S.F., 2005a, The Phanerozoic record of global sea-level change: Science, v. 310, p. 1293–1298, doi: 10.1126/science.1116412.

Miller, K.G., Wright, J.D., and Browning, J.V., 2005b, Visions of ice sheets in a greenhouse world: Marine Geology, v. 217, p. 215–231, doi: 10.1016/j.margeo.2005.02.007.

Murray, J.W., 1991, Ecology and palaeoecology of benthic foraminifera: Essex, UK, Longman Scientific and Technical, 365 p.

Nelson, C.S., and Cook, P.J., 2001, History of oceanic front development in the New Zealand sector of the Southern Ocean during the Cenozoic—A synthesis: New Zealand Journal of Geology and Geophysics, v. 44, p. 535–553.

Nocchi, M., Parisi, G., Monaco, P., Monechi, S., Madile, M., Napoleone, G., Ripepe, M., Orlando, M., Premoli Silva, I., and Bice, D.M., 1986, The Eocene-Oligocene boundary in the Umbrian pelagic sequences, Italy, *in* Pomerol, C., and Premoli Silva, I., eds., Terminal Eocene events: Developments in palaeontology and stratigraphy, Volume 9: Amsterdam, Elsevier, p. 24–40.

Olsson, R.K., and Wise, S.W., 1987, Upper Paleocene to middle Eocene depositional sequences and hiatuses in the New Jersey Atlantic margin, *in* Ross, C., and Haman, D., eds., Timing and depositional history of eustatic sequences: Constraints on seismic stratigraphy: Cushman Foundation for Foraminiferal Research Special Publication 24, p. 99–112.

Olsson, R.K., Miller, K.G., and Ungrady, T.E., 1980, Late Oligocene transgression of middle Atlantic coastal plain: Geology, v. 8, p. 549–554, doi: 10.1130/0091-7613(1980)8<549:LOTOMA>2.0.CO;2.

Owens, J.P., Bybell, L.M., Paulachok, G., Ager, T.A., Gonzalez, V.M., and Sugarman, P.J., 1988, Stratigraphy of the Tertiary sediments in a 945-foot-deep core hole near Mays Landing in the southeastern New Jersey coastal plain: U.S. Geological Survey Professional Paper 1484, 39 p.

Pälike, H., Moore, T., Backman, J., Raffi, I., Lanci, L., Parés, J.M., and Janecek, T., 2005, Integrated stratigraphic correlation and improved composite depth scales for ODP Sites 1218 and 1219, *in* Wilson, P.A., et al., Proceedings of the Ocean Drilling Program, Scientific results, Volume 199:<http://www-odp.tamu.edu/publications/199_SR/213/213.htm>.

Pasley, M.A., and Hazel, J.E., 1990, Use of organic petrology and graphic correlation of biostratigraphic data in sequence stratigraphic interpretations: Examples from the Eocene-Oligocene boundary section, St. Stephens Quarry, Alabama: Gulf Coast Association of Geological Societies Transactions, v. 40, p. 661–683.

Pearson, P.N., Ditchfield, P.W., Singano, J., Harcourt-Brown, K.G., Nicholas, C.J., Olsson, R.K., Shackleton, N.J., and Hall, M.A., 2001, Warm tropical sea surface temperatures in the Late Cretaceous and Eocene epochs: Nature, v. 413, p. 481–487, doi: 10.1038/35097000.

Pekar, S., Miller, K.G., and Browning, J.V., 1997, New Jersey Coastal Plain Oligocene sequences, *in* Miller, K.G., and Snyder, S.W., Proceedings of the Ocean Drilling Program, Scientific results, Volume 150X: College Station, Texas, Ocean Drilling Program, p. 187–206.

Pekar, S.F., Christie-Blick, N., Kominz, M.A., and Miller, K.G., 2001, Evaluating the stratigraphic response to eustasy from Oligocene strata in New Jersey: Geology, v. 29, p. 55–58, doi: 10.1130/0091-7613(2001)029<0055:ETSRTE>2.0.CO;2.

Pekar, S.F., Christie-Blick, N., Kominz, M.A., and Miller, K.G., 2002, Calibration between glacial eustasy and oxygen isotopic data for the early icehouse world of the Oligocene: Geology, v. 30, p. 903–906, doi: 10.1130/0091-7613(2002)030<0903:CBEEFB>2.0.CO;2.

Pitman, W.C., 1978, Relationship between eustacy and stratigraphic sequences on passive margins: Geological Society of America Bulletin, v. 89, p. 1389–1403, doi: 10.1130/0016-7606(1978)89<1389:RBEASS>2.0.CO;2.

Pomerol, C., and Premoli Silva, I., 1986, The Eocene-Oligocene transition: Events and boundary, *in* Pomerol, C., and Premoli Silva, I., eds., Terminal Eocene events: Developments in palaeontology and stratigraphy, Volume 9: Amsterdam, Elsevier, p. 1–24.

Poore, R.Z., and Bybell, L.M., 1988, Eocene to Miocene biostratigraphy of New Jersey core ACGS #4: Implications for regional stratigraphy: U.S. Geological Survey Professional Paper 1829, 22 p.

Posamentier, H.W., Jervey, M.T., and Vail, P.R., 1988, Eustatic controls on clastic deposition I—Conceptual framework, *in* Wilgus, C.K., et al., eds., Sea level changes: An integrated approach: Society of Economic Paleontologists and Mineralogists Special Publication 42, p. 109–123.

Premoli Silva, I., and Jenkins, D.G., 1993, Decision on the Eocene-Oligocene boundary stratotype: Episodes, v. 16, p. 379–382.

Reynolds, D.J., Steckler, M.S., and Coakley, B.J., 1991, The role of the sediment load in sequence stratigraphy: The influence of flexural isostasy and compaction: Journal of Geophysical Research, v. 96, p. 6931–6949.

Savin, S.M., Douglas, R.G., and Stehli, F.G., 1975, Tertiary marine paleotemperatures: Geological Society of America Bulletin, v. 86, p. 1499–1510, doi: 10.1130/0016-7606(1975)86<1499:TMP>2.0.CO;2.

Shackleton, N.J., and Kennett, J.P., 1975, Paleotemperature history of the Cenozoic and initiation of Antarctic glaciation: Oxygen and carbon isotopic analyses in DSDP Sites 277, 279, and 281, *in* Initial reports of the Deep Sea Drilling Project, Volume 29: Washington, D.C., U.S. Government Printing Office, p. 743–755.

Shackleton, N.J., Hall, M.A., and Boersma, A., 1984, Oxygen and carbon isotope data from Leg 74 foraminifers, *in* Moore, T.C., et al., Initial reports of the Deep Sea Drilling Project, Volume 29: Washington, D.C., U.S. Government Printing Office, p. 599–612.

Tauxe, L.P., and Hartl, P., 1997, 11 million years of Oligocene geomagnetic field behavior: Geophysical Journal International, v. 128, p. 217–229, doi: 10.1111/j.1365-246X.1997.tb04082.x.

Tew, B.H., 1992, Sequence stratigraphy, lithofacies relationships, and paleogeography of Oligocene strata in southeastern Mississippi and southwestern Alabama: Geological Survey of Alabama Bulletin, v. 146, p. 1–73.

Tew, B.H., and Mancini, E.A., 1995, An integrated stratigraphic model for paleogeographic reconstruction: Examples from the Jackson and Vicksburg Groups of the eastern Gulf Coastal Plain: Palaios, v. 10, p. 133–153, doi: 10.2307/3515179.

Thomas, E., 1992, Middle Eocene–late Oligocene bathyal benthic foraminifera (Weddell Sea): Faunal changes and implications for ocean circulation, *in* Prothero, D.R., and Berggren, W.A., eds., Late Eocene–Oligocene climatic and biotic evolution: Princeton, New Jersey, Princeton University Press, 245–271.

Tjalsma, R.C., and Lohmann, G.P., 1983, Paleocene-Eocene bathyal and abyssal benthic foraminifera from the Atlantic Ocean: Micropaleontology, Special Publication 4, 90 p.

Toulmin, L.D., 1977, Stratigraphic distribution of Paleocene and Eocene fossils in the eastern Gulf Coast region: Alabama Geological Survey Monograph 13, 602 p.

Tripati, A., Backman, J., Elderfield, H., and Ferretti, P., 2005, Eocene bipolar glaciation associated with global carbon cycle changes: Nature, v. 436, p. 341–346, doi: 10.1038/nature03874.

Vail, P.R., Mitchum, R.M., Jr., Todd, R.G., Widmier, J.M., Thompson, S., III, Sangree, J.B., Bubb, J.N., and Hatlelid, W.G., 1977, Seismic stratigraphy and global changes of sea level, *in* Payton, C.E., ed., Seismic stratigraphy—Applications to hydrocarbon exploration: American Association of Petroleum Geologists Memoir 26, p. 49–212.

Vail, P.R., Colin, J.P., Chène, R.J., Kuchly, J., Mediavilla, F., and Trifilieff, V., 1987, La stratigraphie séquentielle et son application aux corrélations chronostratigraphiques dans le Jurassique du bassin de Paris: Bulletin de la Société Géologique de France, v. 7, p. 1301–1321.

Van Andel, T.H., Heath, G.R., and Moore, T.C., 1975, Cenozoic history and Paleooceanography of the central equatorial pacific: A regional synthesis of Deep See Drilling Project data: Geological Society of America Memoir 143, 34 p.

van Fossen, M., 1997, Magnetostratigraphy of lower Eocene to lower Miocene sediments in cores from the New Jersey coastal plain, *in* Miller, K.G., and Snyder, S.W., Proceedings of the Ocean Drilling Program, Scientific results, Volume 150X: College Station, Texas, Ocean Drilling Program, p. 295–304.

van Morkhoven, F.P.C.M., Berggren, W.A., and Edwards, A.S., 1986, Cenozoic cosmopolitan deep-water benthic foraminifera: Centres de Recherches Exploration-Production Elf-Aquitaine Mémoire 11, 421 p.

Van Sickel, W.A., Kominz, M.A., Miller, K.G., and Browning, J.V., 2004, Late Cretaceous and Cenozoic sea-level estimates: Backstripping analysis of borehole data, onshore New Jersey: Basin Research, v. 16, p. 451–465, doi: 10.1111/j.1365-2117.2004.00242.x.

Watts, A.B., 1981, The U.S. Atlantic continental margin; Subsidence history, crustal structure, and thermal evolution, *in* Bally, A.W., ed., Geology of passive continental margins: History, structure, and sedimentologic record: American Association of Petroleum Geologists Education Course Note Series, v. 19, p.p. 2-i-2–70.

Watts, A.B., and Steckler, M.S., 1979, Subsidence and eustasy at the continental margin of eastern North America, *in* Talwani, M., et al., eds., Deep drilling results in the Atlantic Ocean: Continental margins and paleoenvironment: American Geophysical Union Maurice Ewing series 3, p. 218–234.

Zachos, J.C., Breza, J., and Wise, S.W., 1992, Earliest Oligocene ice-sheet expansion on East Antarctica: Stable isotope and sedimentological data from Kerguelen Plateau: Geology, v. 20, p. 569–573, doi: 10.1130/0091-7613(1992)020<0569:EOISEO>2.3.CO;2.

Zachos, J.C., Stott, L.D., and Lohmann, K.C., 1994, Evolution of early Cenozoic marine temperatures: Paleoceanography, v. 9, p. 353–387, doi: 10.1029/93PA03266.

Zachos, J.C., Quinn, T.M., and Salamy, S., 1996, High resolution ($10^4$ yr) deep-sea foraminiferal stable isotope records of the earliest Oligocene climate transition: Paleoceanography, v. 11, p. 261–266.

Zachos, J., Pagani, M., Sloan, L., Thomas, E., and Billups, K., 2001, Trends, rhythms, and aberrations in global climate 65 Ma to present: Science, v. 292, p. 686–693, doi: 10.1126/science.1059412.

Manuscript received 16 september 2006
Revised manuscript received 18 april 2007
Manuscript accepted 3 may 2007

Printed in the USA